The Plant Cell, Vol. 25: 83–101, January 2013, www.plantcell.org

Transcription Repressor HANABA TARANU Controls Flower Development by Integrating the Actions of Multiple Hormones, Floral Organ Specification Genes, and GATA3 Family Genes in *Arabidopsis*[W]

Xiaolan Zhang,[a,b,c,1,2] Yun Zhou,[b,1] Lian Ding,[a,c] Zhigang Wu,[d] Renyi Liu,[d] and Elliot M. Meyerowitz[b]

[a] College of Agronomy and Biotechnology, China Agricultural University, Beijing 100193, People's Republic of China
[b] Division of Biology, California Institute of Technology, Pasadena, California 91125
[c] Beijing Key Laboratory of Growth and Developmental Regulation for Protected Vegetable Crops, China Agricultural University, Beijing100193, People's Republic of China
[d] Department of Botany and Plant Sciences, University of California, Riverside, California 92521

Plant inflorescence meristems and floral meristems possess specific boundary domains that result in proper floral organ separation and specification. *HANABA TARANU* (*HAN*) encodes a boundary-expressed GATA3-type transcription factor that regulates shoot meristem organization and flower development in *Arabidopsis thaliana*, but the underlying mechanism remains unclear. Through time-course microarray analyses following transient overexpression of *HAN*, we found that HAN represses hundreds of genes, especially genes involved in hormone responses and floral organ specification. Transient overexpression of *HAN* also represses the expression of *HAN* and three other GATA3 family genes, *HANL2* (*HAN-LIKE 2*), *GNC* (*GATA*, *NITRATE-INDUCIBLE*, *CARBON-METABOLISM-INVOLVED*), and *GNL* (*GNC-LIKE*), forming a negative regulatory feedback loop. Genetic analysis indicates that *HAN* and the three GATA3 family genes coordinately regulate floral development, and their expression patterns are partially overlapping. HAN can homodimerize and heterodimerize with the three proteins encoded by these genes, and HAN directly binds to its own promoter and the *GNC* promoter in vivo. These findings, along with the fact that constitutive overexpression of HAN produces an even stronger phenotype than the loss-of-function mutation, support the hypothesis that HAN functions as a key repressor that regulates floral development via regulatory networks involving genes in the GATA3 family, along with genes involved in hormone action and floral organ specification.

INTRODUCTION

Flower formation is a fundamental feature of angiosperm plants and has attracted intensive study in the past decades. Flowers arise from a specialized structure in the shoot tip called the shoot apical meristem (SAM), which comprises a pool of stem cells that continuously divide and replenish themselves (Fletcher, 2002). Despite the fact that flowers display an enormous diversity of morphology in different plants, most flowers have four types of floral organs arranged in concentric whorls, specifically sepals in whorl 1, petals in whorl 2, stamens in whorl 3, and carpels in whorl 4. For a particular plant species, the floral organ number, size, shape, and the relative spatial position are generally fixed.

In *Arabidopsis thaliana*, floral organ identity is specified by the combinatorial actions of three classes of genes, termed A, B, and C, that act in developing floral meristems. A function (provided in part by the *APETALA1* and *APETALA2* genes) determines sepal identity; B function (provided by the *APETALA3* and *PISTILLATA* genes), along with A function, determines petal identity; B function plus C (provided by the *AGAMOUS* gene) determines stamen identity; and C function determines carpel identity (Bowman et al., 1991; Coen and Meyerowitz, 1991; Weigel and Meyerowitz, 1994). In addition to organ identity genes, floral architecture is also affected by genes that function in meristem activity or/and boundary formation. For example, the *CLAVATA* genes (*CLV1*, *CLV2*, and *CLV3*), *PERIANTHIA* (*PAN*), *WUSCHEL* (*WUS*), *SHOOT MERISTEMLESS* (*STM*), and *UNUSUAL FLORAL ORGANS* (*UFO*) largely function in the meristem to regulate floral organ number and shape. Mutation of *CLV* or *PAN* results in increased floral organ number; by contrast, mutation of *WUS*, *STM*, or *UFO* generates flowers with reduced numbers of organs (Long et al., 1996; Clark et al., 1997; Mayer et al., 1998; Chuang et al., 1999; Fletcher et al., 1999; Durfee et al., 2003). On the other hand, *SUPERMAN*, *RABBIT EARS* (*RBE*), *CUP-SHAPED COTYLEDON* (*CUC*), *PETAL LOSS*, and *BLADE-ON-PETIOLE* (*BOP*), whose expression is mainly in the meristem-organ boundary regions, the organ-organ boundary regions, or both, function by establishing proper boundaries to regulate organ number, shape, separation, and relative position (Sakai et al., 1995; Aida et al., 1997; Vroemen

[1] These authors contributed equally to this work.
[2] Address correspondence to zhxiaolan@cau.edu.cn.
The author responsible for distribution of materials integral to the findings presented in this article in accordance with the policy described in the Instructions for Authors (www.plantcell.org) is: Xiaolan Zhang (zhxiaolan@cau.edu.cn).
[W] Online version contains Web-only data.
www.plantcell.org/cgi/doi/10.1105/tpc.112.107854

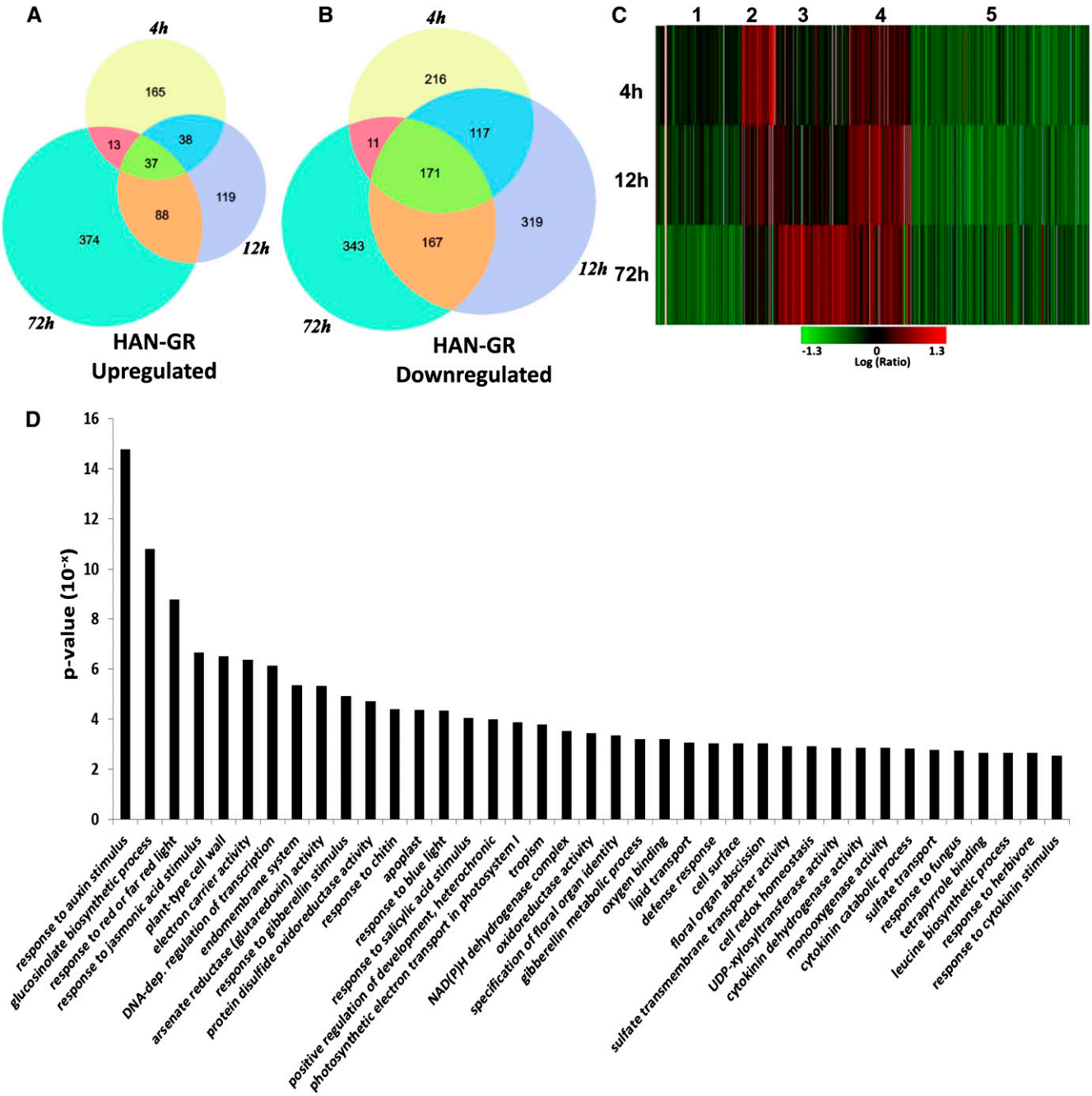

Figure 1. Genome-Wide Transcription Analysis upon Time-Course Induction of *HAN* in the Floral Buds of *35S-HAN-GR Arabidopsis*.

(A) and **(B)** Venn diagrams of differentially expressed genes that were significantly upregulated **(A)** or downregulated **(B)** (P value < 0.001, fold change >2 or <−2) 4, 12, and 72 h after DEX induction of *HAN*.

(C) Clustering displays of expression ratios (DEX treatment versus mock-treated control) for genes that are differentially expressed in at least one of the time points (4, 12, or 72 h). Red color indicates upregulation and green indicates downregulation.

(D) GO terms that are significantly enriched (P < 0.003) in cluster 5. GO terms were sorted based on P value.

et al., 2003; Brewer et al., 2004; Takeda et al., 2004; Hepworth et al., 2005).

HANABA TARANU (*HAN*) is expressed at the boundaries between meristem and organ primordia and at the boundaries between different floral organs (Zhao et al., 2004). *HAN* knockouts display small, flat SAMs, fused sepals, and reduced numbers of floral organs, whereas *HAN* overexpression leads to delayed plant growth, disturbed cell division, and loss of meristem activity (Zhao et al., 2004). HAN also plays an important role in proembryo boundary formation through regulation of auxin flux and

establishing cotyledon identity during embryogenesis in *Arabidopsis* (Nawy et al., 2010; Kanei et al., 2012). The gene expression domain and function of *HAN* are not conserved between monocots and dicots. In the grass family, *HAN* homologs such as *TASSEL SHEATH* (*TSH*) in maize (*Zea mays*), *NECK LEAF1* (*NL1*) in rice (*Oryza sativa*), and *THIRD OUTER GLUME* (*TRD*) in barley (*Hordeum vulgare*) are expressed similarly in the cells of the suppressed bract, and loss of function of *TSH*/*NL1*/*TRD* results in bract outgrowth (Wang et al., 2009; Whipple et al., 2010).

HAN belongs to a family of 30 members in *Arabidopsis* that code for GATA3–type transcription factors that have a single zinc finger domain (Zhao et al., 2004; Bi et al., 2005). GATA factors were initially named for their ability to bind the consensus DNA sequence WGATAR (W = T or A; R = G or A) (Lowry and Atchley, 2000). In animals, GATA factors have been shown to act in development, differentiation, and cell proliferation (Patient and McGhee, 2002), whereas fungal GATA factors participate in nitrogen metabolism, circadian regulation, mating-type switching, and light-regulated photomorphogenesis (Scazzocchio, 2000). In plants, GATA factors have been identified to regulate both developmental processes and responses to environmental stimuli, such as light signaling, circadian rhythms, photoperiodic control of flowering, seed germination, brassinosteroid signaling, lateral root founder cell specification, and stress responses (Putterill et al., 1995; Teakle et al., 2002; Sugimoto et al., 2003; Liu et al., 2005; De Rybel et al., 2010; Luo et al., 2010). GNC (for GATA, NITRATE-INDUCIBLE, CARBON-METABOLISM-INVOLVED) and GNL (for GNC-LIKE) are two GATA transcription factors that belong to the same subfamily II as HAN in *Arabidopsis* (Reyes et al., 2004). GNC and GNL have been shown to mediate nitrogen metabolism, chlorophyll biosynthesis, and glucose sensitivity (Bi et al., 2005). Furthermore, *GNC* and *GNL* are directly repressed by floral homeotic genes *APETALA3* and *PISTILLATA* during flower development and are important repressors of gibberellin signaling that regulate germination, greening, flowering time, and leaf elongation (Bi et al., 2005; Mara and Irish, 2008; Richter et al., 2010). However, little is known about the potential interactions between plant GATA family members, and little if anything is known about the underlying mechanism by which boundary-expressed *HAN* regulates floral organ development.

Here, we show that transient overexpression of *HAN* causes large-scale gene repression, especially repression of genes that are involved in hormone responses and floral organ specification. Induction of *HAN* also leads to negative autoregulation and repression of three additional GATA3 family genes: *HAN-LIKE2* (*HANL2*), *GNC*, and *GNL*. Genetic analyses indicate that *HAN* and other GATA3 family genes coordinately regulate sepal separation, petal number, silique length, and stamen and embryo development. Transcripts of *HANL2*, *GNC*, and *GNL* have similar accumulation patterns that are partially overlapping with the expression pattern of *HAN*. We further show that HAN can homodimerize and heterodimerize with GATA3 family proteins and that HAN directly binds to its own promoter and the promoter of *GNC* in vivo. Our results suggest that HAN may function as a key

Table 1. qRT-PCR Corroboration of Differentially Expressed Genes under Transient Overexpression of HAN

Gene ID	Gene Name	P Value	Microarray DEX, Fold Change	qRT-PCR Fold Change	*han-1* Fold Change[a]
At1g74890	ARR15	4.1E-26	–3.40[b]	–4.92 ± 1.20	–1.86 ± 0.19
At1g66350	RGL1	0.0E+00	–3.80[b]	–3.23 ± 0.43	–1.39 ± 0.08
At3g23050	IAA7	0.0E+00	–2.10[b]	–1.68 ± 0.55	–1.70 ± 0.06
At3g10000	EMBRYO SAC DEVELOPMENT ARREST31 (EDA31)	5.4E-07	–5.20[b]	–7.06 ± 1.29	–1.40 ± 0.03
At4g32980	*ARABIDOPSIS THALIANA* HOMEOBOX GENE1 (ATH1)	3.5E-09	–2.30[b]	–5.04 ± 1.23	–4.39 ± 1.24
At1g70510	KNAT2	4.1E-14	–2.40[b]	–3.57 ± 1.25	–1.00 ± 0.16
At5g11060	KNAT4	0.0E+00	–3.90[b]	–2.24 ± 0.30	–4.22 ± 0.03
At1g24260	SEP3	2.5E-20	–2.20[b]	–2.21 ± 0.15	–2.19 ± 0.33
At1g69530	ATEXPA1	0.0E+00	–3.90[b]	–2.52 ± 0.55	–1.45 ± 0.06
At1g01470	LATE EMBRYOGENESIS ABUNDANT PROTEIN14 (LEA14)	3.3E-19	2.90[b]	2.10 ± 0.23	–2.60 ± 0.53
At1g51950	IAA18	8.0E-07	–2.00[c]	–2.04 ± 0.27	–4.15 ± 0.67
At5g13220	JAZ10	1.3E-10	–2.60[c]	–6.85 ± 0.90	–4.92 ± 0.19
At2g34600	JAZ7	4.9E-26	–3.30[c]	–2.81 ± 0.65	–5.82 ± 1.40
At2g45190	ABNORMAL FLORAL ORGANS (AFO)	1.4E-35	–2.70[c]	–5.95 ± 0.10	–2.64 ± 0.38
At3g26790	FUS3	4.8E-10	–4.80[c]	–1.11 ± 0.37	–2.36 ± 0.53
At2g21650	MATERNAL EFFECT EMBRYO ARREST3 (MEE3)	2.2E-05	–3.20[c]	–7.11 ± 1.31	2.23 ± 0.03
At1g70210	CYCD1;1	0.0E+00	–3.70[c]	–5.37 ± 1.99	–1.46 ± 0.06
At1g59940	ARR3	1.3E-07	4.00[c]	4.46 ± 0.86	–1.83 ± 0.17
At3g48100	ARR5	5.7E-31	4.00[c]	1.70 ± 0.11	–1.19 ± 0.06
At5g06070	RBE	7.8E-09	2.10[c]	1.60 ± 0.37	–2.67 ± 0.02

[a]Fold change presented as relative abundance of transcripts in han1/wild-type L*er* floral buds.
[b]Fold change at 4 h interval
[c]Fold change at 72 h interval

Table 2. Examples of hormone action genes that are differentially expressed in the 35S-HAN-GR flowers in DEX-treated samples vs. mock-treated controls

		Fold Change			
Gene ID	Gene Name	4h	12h	72h	Cluster
Auxin response					
At1g19220	ARF19 (AUXIN RESPONSE FACTOR 19)	–2.4	–1.8	–2.1	5
At3g04730	IAA16 (INDOLE-3-ACETIC ACID INDUCIBLE16)	–5.3	–3.2	–2.0	5
At1g51950	IAA18 (INDOLE-3-ACETIC ACID INDUCIBLE18)	–1.5	–2.0	–2.0	5
At3g17600	IAA31 (INDOLE-3-ACETIC ACID INDUCIBLE31)	–2.0	–2.3	–1.9	5
At2g01200	IAA32 (INDOLE-3-ACETIC ACID INDUCIBLE32)	–2.0	–2.5	–1.5	5
At1g52830	IAA6 (INDOLE-3-ACETIC ACID INDUCIBLE6)	–2.0	–2.1	3.5	5
At3g23050	IAA7 (INDOLE-3-ACETIC ACID INDUCIBLE7)	–2.1	–3.0	–2.0	5
At1g29510	SAUR68 (SMALL AUXIN UPREGULATED 68)	–4.4	–4.5	–3.3	5
At5g63160	BT1 (BTB AND TAZ DOMAIN PROTEIN 1)	–1.8	–2.3	–2.0	5
At4g37390	YDK1 (YADOKARI-1)	3.2	2.0	–1.5	2
At3g07390	AIR12 (AUXIN-INDUCED PROTEIN12)	2.5	1.2	1.1	2
At4g27260	GH3.5 (Auxin-responsive GH3 family protein)	3.6	3.4	1.7	4
At1g12980	DRN(DORNROSCHEN)	1.1	3.3	1.6	4
Jasmonate response					
At1g32640	MYC2 (bHLH DNA-binding family protein)	–1.7	–2.2	–1.3	5
At3g17860	JAZ3 (JASMONATE-ZIM-DOMAIN PROTEIN 3)	–1.9	–2.3	–1.5	5
At1g17380	JAZ5 (JASMONATE-ZIM-DOMAIN PROTEIN 5)	–1.3	–2.2	–1.2	5
At2g34600	JAZ7 (JASMONATE-ZIM-DOMAIN PROTEIN 7)	–2.7	–2.7	–3.3	5
At5g13220	JAZ10 (JASMONATE-ZIM-DOMAIN PROTEIN 10)	–2.4	–2.5	–2.6	5
At4g23600	CORI3 (CORONATINE INDUCED 3)	–2.7	–5.2	–20.5	5
At3g45140	LOX2 (LIPOXYGENASE 2)	–2.0	–6.4	–7.7	5
At5g47220	ERF2 (ETHYLENE RESPONSIVE ELEMENT BINDING FACTOR 2)	–1.5	–3.1	–1.4	5
Gibberellin response					
At1g14920	GAI (GA INSENSITIVE)	–2.3	–2.9	–2.1	5
At1g66350	RGL1 (RGA-LIKE1)	–3.8	–3.9	–3.1	5
At5g15230	GASA4 (GAST1 PROTEIN HOMOLOG 4)	–2.6	–5.2	–2.8	5
At5G59780	MYB59 (MYB DOMAIN PROTEIN 59)	–2.2	–3.8	–1.9	5
At5g61420	MYB28 (MYB DOMAIN PROTEIN 28)	–2.0	–3.8	–3.8	5
At4g36410	UBC17 (UBIQUITIN CONJUGATING ENZYME 17)	–3.6	–3.1	–1.6	5
At1g68320	MYB62 (MYB DOMAIN PROTEIN 62)	–1.8	–2.2	–3.4	5
Cytokinin response					
At1g74890	ARR15 (RESPONSE REGULATOR 15)	–3.4	–3.2	–2.6	5
At1g59940	ARR3 (RESPONSE REGULATOR 3)	–1.1	1.2	4.0	3
At3g48100	ARR5 (RESPONSE REGULATOR 5)	–1.8	1.6	4.0	3
At5g62920	ARR6 (RESPONSE REGULATOR 6)	–1.1	2.8	3.3	3
At1g19050	ARR7 (RESPONSE REGULATOR 7)	–4.7	–1.9	–1.4	5
At5g56970	CKX3 (CYTOKININ OXIDASE 3)	–4.1	–5.0	–16.5	5
At3g16360	AHP4 (ARABIDOPSIS HISTIDINE-CONTAINING PHOSPHOTRANSFER FACTOR 4)	–5.0	–3.6	–3.9	5

repressor that regulates floral development via regulatory networks involving genes in the GATA3 family, hormone action, and floral organ specification.

RESULTS

Genome-Wide Transcription Analyses upon Inducible Overexpression of *HAN*

To dissect the molecular function of *HAN*, we performed time-course transcriptome analysis using a full-genome microarray, after the transient induction of *HAN* activity in *p35S:HAN-GR* plants, the same line as previously described (Zhao et al., 2004). Briefly, the *p35S:HAN-GR* line was constructed by inserting the full-length cDNA of *HAN* (no stop codon) into the pGreen 0229 vector containing a 2X35S promoter, a glucocorticoid receptor (GR) fragment (conferring resistance to dexamethasone [DEX]), and a *nopaline synthase* terminator (Zhao et al., 2004). Plants were treated with 10 μM DEX, and inflorescences containing flower buds from stages 1 to 9 were collected for microarray assays from plants at 4, 12, and 72 h after the initial DEX treatments and corresponding mock treatments. We identified 2074 genes that showed significantly differential expression ($P < 0.001$ and fold change > 2 or < -2) under DEX treatment in at least one of the three time points ($q < 0.009$) (see Supplemental Data Set 1 online). Although the numbers of upregulated genes

and downregulated genes were similar after 72 h of induction, downregulated genes outnumbered upregulated genes significantly at the early time points of *HAN* induction. The numbers of upregulated genes were 253 and 282, and the numbers of downregulated genes were 515 and 774 after 4- and 12-h treatments, respectively. Moreover, there are many more shared downregulated genes than upregulated genes (88 shared up versus 444 shared down) (Figures 1A and 1B). To further understand the dynamic trend of these RNA abundances after *HAN* induction, we clustered genes with similar expression patterns across the three time points. As shown in Figure 1C, genes that showed differential expression in at least one time point can be grouped into five clusters. Genes in clusters 1 and 5 were downregulated in the HAN induction samples compared with the controls, whereas genes in the other three clusters were upregulated. Cluster 1 genes are repressed, and cluster 3 genes are activated only at 72 h, suggesting that these are probably late effects of HAN induction. Cluster 2 genes were induced only at 4 h and later returned to their normal expression levels, indicating that they may be stress-responsive genes. By contrast, clusters 4 and 5 likely reveal the specific mechanisms of HAN-mediated transcriptional regulation. Cluster 4 genes were weakly upregulated at 4 h, reached highest induction at 12 h, and returned to weak upregulation at 72 h. Cluster 5 genes were greatly repressed at 4 h and maintained this repression later on, suggesting that these genes may be the direct targets of HAN. Cluster 5 is the biggest group and accounts for over 40% of all the differentially expressed genes (Figure 1C; see Supplemental Data Set 1 online), implicating HAN as a master repressor that downregulates the transcription of a large numbers of genes.

Quantitative RT-PCR Corroboration of Differentially Expressed Genes under Transient Overexpression of HAN

To verify the differentially expressed genes identified by microarray, we performed quantitative RT-PCR (qRT-PCR) using independently generated DEX-treated versus mock-treated *p35S*:*HAN-GR* flowers (Table 1). Among the 20 genes we tested, 16 genes showed the same differential expression in the DEX-treated sample, and the other four genes also displayed the same patterns as those observed in microarray analysis, although the quantitative fold change in the qRT-PCR experiment was smaller than a twofold cutoff. The qRT-PCR and microarray data exhibited close agreement (Pearson correlation coefficient was 0.80, P = 1.4E-05) in the fold change between DEX-treated and mock-treated samples, indicating that the microarray data are reliable.

HAN Regulates Flower Development via Hormone Action and Floral Organ Regulatory Networks

To analyze the functions of the differentially expressed genes upon *HAN* induction, we performed Gene Ontology (GO) term enrichment analysis for each cluster. In addition to the metabolic and stress-related pathways that were identified in all clusters, hormone action and floral organ regulators are significantly enriched in cluster 5 (Figure 1D, Tables 2 and 3; see Supplemental Figure 1 online). The most significantly enriched GO term is "response to auxin stimulus" ($P < 10^{-14}$). Accordingly, lists of three well-known groups of early auxin-responsive genes including the auxin/indole-3-acetic acid (*Aux/IAA*), the *small auxin-up RNA* (*SAUR*), and the *GH3* gene families are differentially expressed upon *HAN* overexpression (Wang et al., 2008) (Figure 1D, Table 2). *IAAs* and *SAURs* are generally repressed, while GH3s are induced by *HAN* overexpression. For example, the expression of IAA16 and SAUR68 decreases 5.3- and 4.4-fold, respectively, and the expression of GH3 family genes *YADOKARI1* (*YDK1*) and *GH3.5* increases 3.2- and 3.6-fold, respectively, upon 4 h DEX-induced HAN treatment (Table 2). We verified the repression of IAA16 and the induction of *GH3.5* by quantitative PCR (see Supplemental Table 1 online). The expression of IAA16 showed no change in *han* mutants versus wild-type plants, while *GH3.5* RNA is reduced in the HAN null allele *han-1* (8.8-fold decrease) (see Supplemental Table 1 online), suggesting that *GH3.5* but not IAA16 may be a direct target of HAN. To further verify whether HAN indeed regulates auxin action during flower development, we introduced the auxin response reporter *pDR5rev*:*3XVENUS-N7* together with the auxin transport marker *pPIN1*:*PIN1-GFP* (for green fluorescent protein) to *han-2* mutant plants (Heisler et al., 2005). The fluorescence from the *pDR5rev*:*3XVENUS-N7* reporter is greatly reduced in the inflorescence meristems (IMs) of the *han-2* mutant plants, especially at the floral primordia, compared with those in Landsberg *erecta* (L*er*). By contrast, the *pPIN1*:*PIN1-GFP* reporter shows no appreciable change in fluorescence in *han-2* (Figure 2). Consistent with our microarray data, live imaging results reveal that HAN mediates auxin response/signaling but not auxin transport during flower development.

Genes that are involved in responses to other hormones, such as jasmonic acid, gibberellin, and cytokinin, are significantly enriched in cluster 5 as well (Figure 1D). For example, the jasmonate signaling genes that encode jasmonate ZIM domain proteins (JAZ3, 5, 7, and 10), MYC2, and CORONATINE INDUCED1 (CORI3) are significantly repressed upon *HAN* induction (Table 2) (Fonseca et al., 2009). The DELLA family genes *GA INSENSITIVE* (*GAI*) and *RGA-LIKE1* (*RGL1*) in the gibberellin signaling and *RESPONSE REGULATOR15* (*ARR15*) and *ARABIDOPSIS HISTIDINE-CONTAINING PHOSPHOTRANSFER FACTOR4* (*AHP4*)

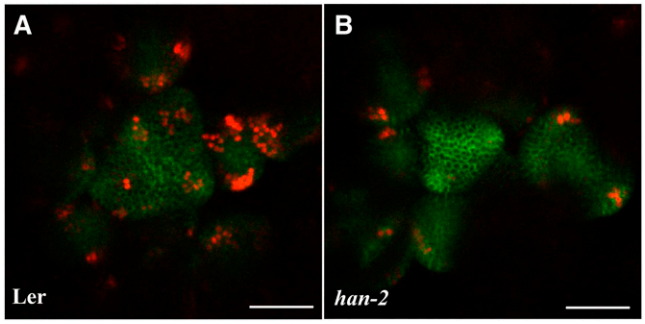

Figure 2. Auxin Response Is Greatly Compromised in *han-2* Mutant Plants.

pDR5rev:*3XVENUS-N7* (red) and *pPIN1*:*PIN1-GFP* (green) markers in wild-type L*er* **(A)** and *han-2* mutant **(B)** IMs. Images are representative of 10 to 20 plants grown under the same environmental conditions. Bars = 50 μm.

Table 3. Examples of developmental regulators that are differentially expressed in the *35S-HAN-GR* flowers in DEX-treated samples vs. mock-treated controls

		Fold Change			
Gene ID	Gene Name	4h	12h	72h	Cluster
Flower development					
At2g41370	BOP2 (BLADE ON PETIOLE2)	–1.5	–2.0	–2.1	5
At3g57130	BOP1 (BLADE ON PETIOLE1)	–2.0	–2.0	–1.3	5
At4g32980	ATH1 (ARABIDOPSIS THALIANA HOMEOBOX GENE 1)	–2.3	–3.2	–1.7	5
At1g24260	SEP3 (SEPALLATA3)	–2.2	–2.1	–1.9	5
At2g45190	AFO (ABNORMAL FLORAL ORGANS)	–2.4	–3.9	–2.7	5
At1g70510	KNAT2 (KNOTTED-LIKE2)	–2.4	–2.5	–1.5	5
At5g11060	KNAT4 (KNOTTED-LIKE4)	–3.9	–2.3	–1.6	5
At4g08150	BP (BREVIPEDICELLUS)	–2.2	–2.8	–1.1	5
At1g68480	JAG (JAGGED)	–1.8	–1.7	–2.1	5
At5g67180	TOE3 (TARGET OF EAT 3)	–2.3	–2.3	–1.8	5
At1g69490	NAP (NAC-LIKE ACTIVATED BY AP3/PI)	2.4	2.3	2.7	4
At5g06070	RBE (RABITT EARS)	1.5	2.6	2.1	4
At1g76420	CUC3 (CUP-SHAPED COTYLEDON 3)	1.4	3.4	1.8	4
Reproductive development					
At3g10000	EDA31 (EMBRYO SAC DEVELOPMENT ARREST 31)	–5.2	–6.2	–4.1	5
At2g21650	MEE3 (MATERNAL EFFECT EMBRYO ARREST 3)	–1.8	–2.5	–3.2	5
At4g21330	DYT1 (DYSFUNCTIONAL TAPETUM 1)	–1.5	–2.3	–3.1	5
At1g01470	LEA14 (LATE EMBRYOGENESIS ABUNDANT PROTEIN)	2.9	4.2	2.1	4
At4g28520	CRU3 (CRUCIFERIN 3)	–1.2	2.0	–3.6	1
At3g26790	FUS3 (FUSCA3)	–1.0	1.3	–4.8	1
Positive regulation of development					
At1g53230	TCP3 (TCP family transcription factor 3)	–1.6	–2.4	–1.8	5
At3g02150	TCP13 (TCP family transcription factor 13)	–2.9	–1.8	–1.2	5
At3g15030	TCP4 (TCP family transcription factor 4)	–1.8	–2.7	–2.2	5
At5g60970	TCP5 (TCP family transcription factor 5)	–2.0	–1.9	–1.5	5
Cell division & expansion					
At1g70210	CYCD1;1 (CYCLIN DELTA-1)	–1.9	–2.0	–3.7	1
At1g69530	ATEXPA1 (ARABIDOPSIS THALIANA EXPANSIN A1)	–3.9	–1.7	–2.0	5
At1g20190	ATEXPA11 (ARABIDOPSIS THALIANA EXPANSIN A11)	–2.7	–2.2	–1.3	5
At5g56320	ATEXPA14 (ARABIDOPSIS THALIANA EXPANSIN A14)	–1.6	–2.4	–2.6	5
At3g29030	ATEXPA5 (ARABIDOPSIS THALIANA EXPANSIN A5)	–2.5	–2.4	–1.2	5
GATA3 family					
At3g50870	HAN (HANABA TARANU)	–1.2	–1.6	–2.0	1
At5g56860	GNC (GATA, NITRATE-INDUCIBLE, CARBON-METABOLISM-INVOLVED)	–2.6	–5.3	–6.6	5
At4g36620	HANL2 (HAN-LIKE2)	–3.3	–3.2	–3.2	5
At4g26150	GNL (GNC LIKE)	1.5	–4.9	–5.1	5

in the cytokinin two-component signaling pathway are also largely downregulated upon transient *HAN* overexpression (Table 2) (Hirano et al., 2008; To and Kieber, 2008). Therefore, HAN seems to function as a negative regulator that mediates multiple hormone response and/or signaling pathways.

In addition, the expression of genes encoding many well-known developmental regulators are significantly altered upon *HAN* induction, including flower developmental genes, such as *BOP1* and *2*, *RBE*, *CUC3*, *BREVIPEDICELLUS* (*BP*), *KNOTTED-LIKE2* (*KNAT2*), and *SEPALLATA3* (*SEP3*), and reproductive development genes, such as *FUSCA3* (*FUS3*) and *DYSFUNCTIONAL TAPETUM1* (*DYT1*), indicating that HAN regulates floral organ and embryo development through the interaction with known developmental regulators (Table 3) (Pelaz et al., 2000; Pautot et al., 2001; Vroemen et al., 2003; Takeda et al., 2004; Tsuchiya et al., 2004; Zhao et al., 2004; Hepworth et al., 2005; Hibara et al., 2006; Zhang et al., 2006). In addition, transient *HAN* overexpression greatly represses the expression of HAN itself and several homologous genes in the same family (Table 3), suggesting a negative regulatory feedback. Therefore, we performed a more detailed characterization of this group of genes.

Repression of GATA3 Family Genes upon Inducible Overexpression of *HAN*

Induction of *HAN* with DEX leads to a progressive reduction of endogenous *HAN* RNA. After 72 h of DEX treatment, the accumulation of HAN transcripts decreases by half compared with the mock-treated plants (Figure 3A, Table 3). Moreover, induction of *HAN* significantly represses the expression of three

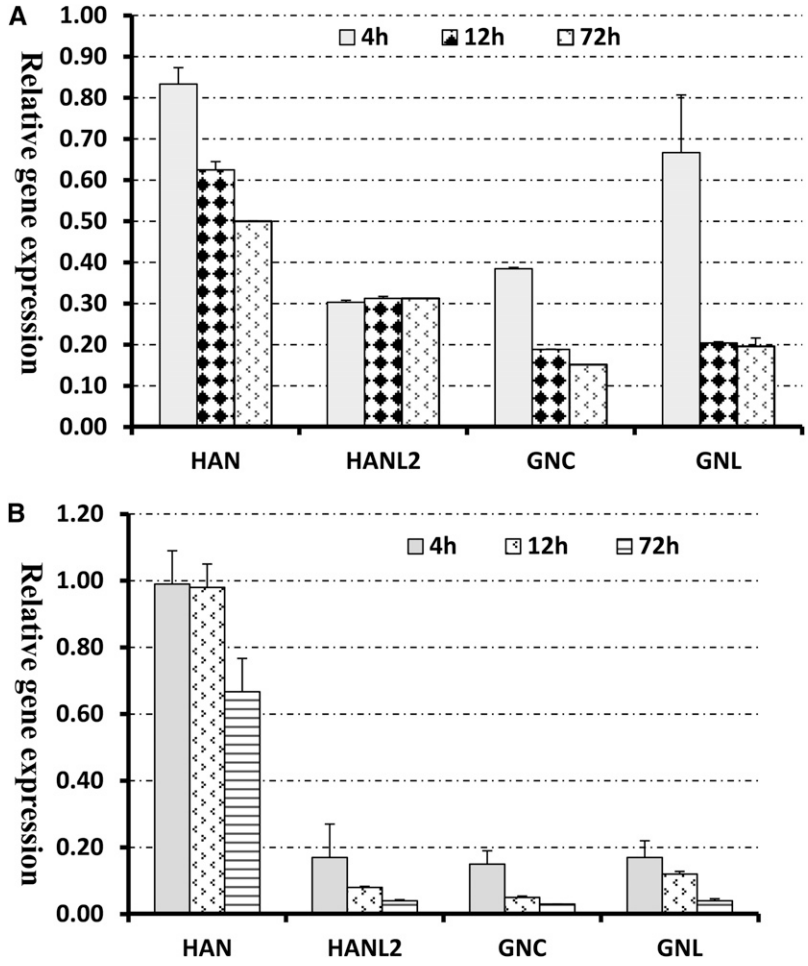

Figure 3. Transient Induction of *HAN* Represses the Transcription of *HAN* and the Three GATA3 Family Genes *HANL2*, *GNC*, and *GNL*.

(A) Microarray analyses of the expression of *HAN* and *GATA3* family genes in the floral buds of the *35S-HAN-GR* line upon DEX treatment. Data are presented as the ratios of expression levels in the DEX-treated samples versus mock-treated samples. Four biological replicates were used for the microarray hybridization.

(B) Transcription analyses by qRT-PCR using independently generated RNA samples. Three biological replicates were used for each time point, and all samples were normalized according to the expression level of Actin2. Error bars represent the SE between biological replicates.

GATA3 family genes: *HANL2*, *GNC*, and *GNL*, which belong to the same subfamily II as *HAN* (Reyes et al., 2004). For simplicity, the term GATA3 family genes will hereafter refer to *HANL2*, *GNC*, and *GNL* collectively. *HANL1* and *HANL2* are the two close homologs of *HAN*, which contain the HAN motif in *Arabidopsis*, and their biological function is unknown (Zhao et al., 2004). After 4 h of DEX treatment, transcripts of *HANL2* decrease by 3.3-fold and subsequently remain at this level, while there is no change in the level of *HANL1* transcripts (Table 3). Similarly, *HAN* induction reduces the levels of *GNC* and *GNL* transcripts as well. After 72 h of DEX treatment, the accumulation of *GNC* and *GNL* transcripts is only 15 and 20% of those in the mock treatments (Table 3). To validate our results and control for potential cross-hybridization between family members in the microarray, we performed quantitative real-time RT-PCR. As shown in Figure 3B, *HAN* overexpression from a transgene indeed results in a progressive repression of RNA accumulation from the endogenous gene and a rapid negative regulation of *HANL2*, *GNC*, and *GNL*. For example, upon 4 h of DEX treatment, *HAN* expression has not changed, whereas transcripts of *HANL2*, *GNC*, and *GNL* decrease by 5.8-, 6.6-, and 5.8-fold, respectively. Upon 72 h DEX treatment, *HAN* expression is reduced to 70% of its starting value, similar to the microarray results, while *HANL2*, *GNC*, and *GNL* transcripts decrease 25-, 33-, and 25-fold respectively compared with the mock-treated samples.

Interactions between HAN and GATA3 Family Genes

To investigate the genetic interactions between HAN and the GATA3 family genes identified in the microarray experiments, we used a weak allele of *HAN* (*han-2*) and T-DNA insertion lines of *HANL2* (SALK_138626), *GNC* (SALK_001778), and *GNL* (SAILK_003995) to generate all possible combinations of double and triple mutants

(Bi et al., 2005). Although single mutants and any combination of double mutants of *GNC*, *GNL*, and *HANL2* had no evident floral developmental phenotypes, double and triple mutants of *HAN* with *GNC*, *GNL*, and *HANL2* showed progressive and synergistic effects on sepal fusion, petal number, fertility defects, and carpel abnormality (Figures 4 and 5). The single *han-2* mutant has reduced silique length, decreased fertility, and fewer sepals, petals, and stamens, and it displays occasional sepal fusion and carpelloid stamens (Zhao et al., 2004). The silique length in the double mutants (*han-2 hanl2*, *han-2 gnc*, and *han-2 gnl*) is decreased ~20%, and seed yields are reduced (see Supplemental Figure 2 online). In the triple mutants (*han-2 hanl2 gnc*, *han-2 hanl2 gnl*, and *han-2 gnc gnl*), the siliques exhibit almost no expansion or elongation, and the plants are almost sterile (Figures 4B and 4C; see Supplemental Figure 2 online). Floral organ development is even more severely affected in the double and triple mutants. The most obvious defect is the reduction of petal number. For example, the single *han-2* mutant usually has three petals, while the average petal number is 1.1 and 0.3 in the *han-2 hanl2* double and *han-2 hanl2 gnc* triple mutant plants, respectively (Figures 4D and 5A). Moreover, there are increases in the frequency of sepal fusion and carpelloid stamens in plants with combined mutations in HAN with GATA3 family genes. The frequency of sepal fusion in the *han-2* single mutant is 7%, while it increases to 47, 47, and 40% in the double mutants *han-2 gnl*, *han-2 hanl2*, and *han-2 gnc*, respectively, and 67, 60, and 37% in the triple mutants *han-2 hanl2 gnl*, *han-2 gnc gnl*, and *han-2 hanl2 gnc*, respectively (Figure 5B). By contrast, stamen/carpel development seems to be mainly regulated by GNC and HAN, double mutations of *GNC* and *HAN* result in an over 12-fold increase in the occurrence of carpelloid stamens compared with *han-2* single mutants, whereas in the *han-2 hanl2* or *han-2 gnl* double mutant plants, the frequency of carpelloid stamens is about the same as in the *han-2* single mutant (Figure 5B). There is no phenotypic difference between homozygous triple mutants and plants with homozygous mutations in *HAN*, homozygous for a second member, and heterozygous for a third member, suggesting functional redundancy among *HANL2*, *GNC*, and *GNL*.

We also compared embryo development in the *han-2* single mutant with development in double and triple mutants. HAN has previously been shown to function during *Arabidopsis* embryo development and is required for proper proembryo boundary position (Zhao et al., 2004; Nawy et al., 2010). As shown in Figure 6, *han-2* embryo development displays some degree of abnormality, such as unequal or partially fused cotyledons, along with slightly disorganized embryo shape and boundary positions. In the double or triple mutants of *HAN* and GATA3 family genes, embryo development is severely disrupted. Most embryos prematurely terminated at the globular stage, after forming

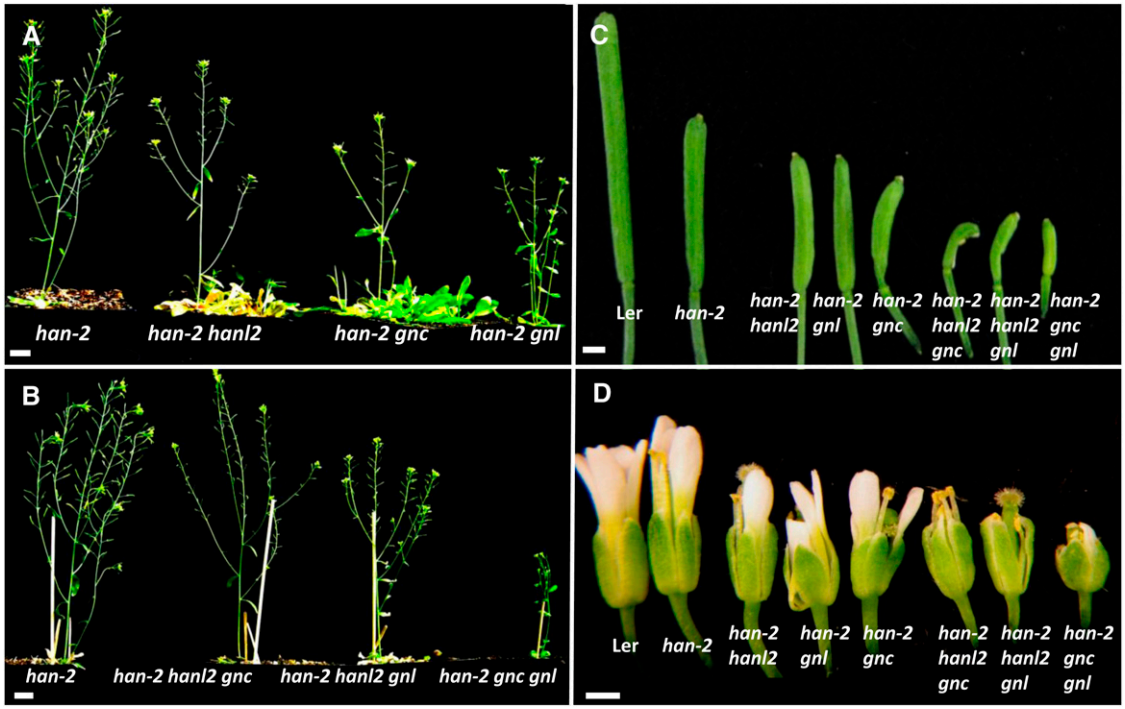

Figure 4. Floral Phenotypes of Mutations in *HAN* and GATA3 Family Genes.

(A) Representative image of a *han-2* single mutant plant and double mutant plants of *HAN* and GATA3 family genes.
(B) Representative image of a *han-2* single mutant plant and triple mutants of HAN and GATA3 family genes.
(C) and **(D)** Silique length **(C)** and floral morphology **(D)** are progressively more defective in higher combinations of mutations of *HAN* and GATA3 family genes.
Bars = 1 cm in **(A)** and **(B)** and 1 mm in **(C)** and **(D)**.

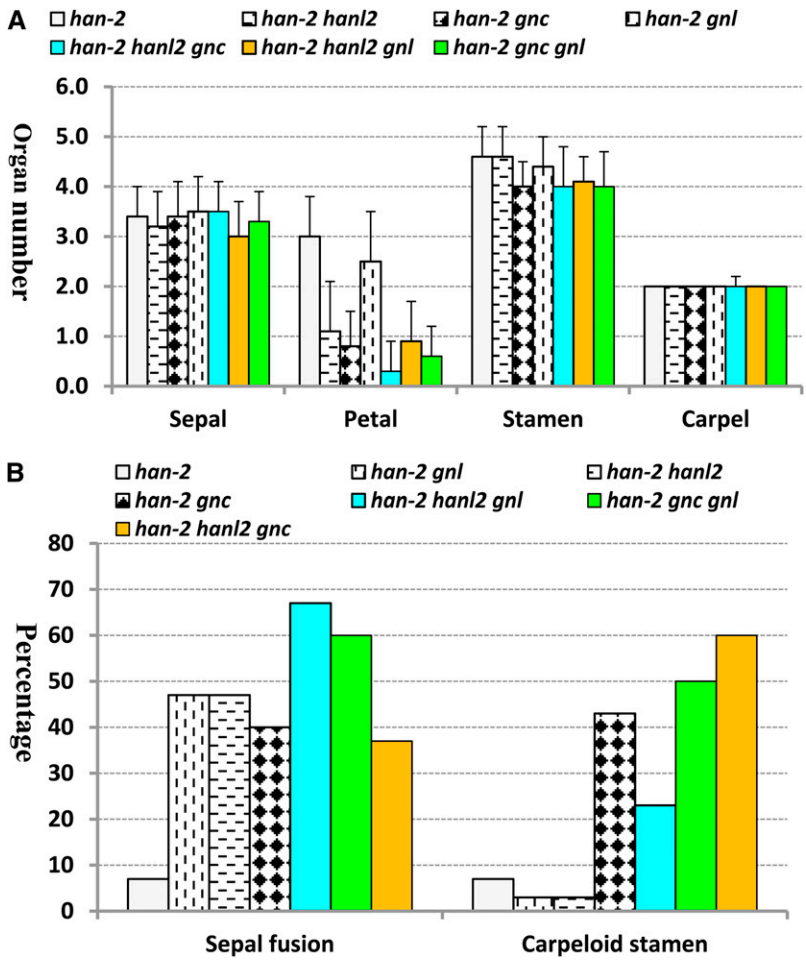

Figure 5. Quantification of Floral Abnormality in GATA3 Family Mutants.

(A) The average floral organ numbers of 30 flowers counted from *han-2* single mutant and all of the combinatory double and triple mutants between HAN and GATA3 family genes. Error bars represent the SD.
(B) The frequency of sepal fusion and carpelloid stamens calculated from 30 flowers of each mutant background.

a cluster of cells, either in a round or irregular shape (Figure 6). Moreover, HAN and GNL may be involved in general plant growth, since the plant height and size decreased greatly when the plants bore combinations of *HAN* and *GNL* mutations (Figures 4A and 4B).

Similar Transcript Accumulation Patterns of *HANL2*, *GNC*, and *GNL*

We next examined the expression patterns of *HANL2*, *GNC*, and *GNL* during flower development by in situ hybridization. We examined the specificity of our probes by hybridizing the HANL2 probe to flowers of a *hanl2* null mutant, SALK_138626 (Bi et al., 2005). As shown in Supplemental Figure 3 online, there is almost no signal in the *hanl2* mutant background, showing that the probe reflects the in vivo transcript accumulation of GATA3 family genes. HANL2 is expressed throughout the IM and early stages of floral primordia (stages 1 to 3) (Figures 7A and 7B). From stage 6 onward, HANL2 is largely restricted to the inner three whorls, specifically in the petals, stamens, and carpels (Figures 7C and 7D). Within the stamens, the strongest expression of HANL2 is detected in the anther locules as well as in the vascular strands, whereas in carpels, the strongest expression is limited to ovules (Figure 7E). The expression patterns of *GNC* and *GNL* overlap with that of *HANL2*, confirming that the three GATA3 family genes may share similar functions. Transcripts of *GNC* and *GNL* are first detected in the IM and young flower buds. As the flowers develop (from stage 6 onward), *GNC* and *GNL* signals are mostly limited to the inner three whorls, which is consistent with data from previous studies (Mara and Irish, 2008) (Figures 7F to 7I and 7K to 7N). Transverse sections showed that *GNC* and *GNL* expression is mainly detectable in the anther locules, vascular strands, and ovules (Figures 7J and 7O). However, the signal intensity of *HANL2*, *GNC*, and *GNL* are different, with *HANL2* having the strongest, *GNL* the intermediate, and GNC the weakest expression in all of the tissues that we examined (Figure 7). Given that transcripts of *HAN* are detected at the boundaries between the meristem and lateral organ primordia, the lateral and basal regions of carpels, and the anther

locules and vascular strands (Zhao et al., 2004), *HAN* partially overlaps with the expression patterns of *HANL2*, *GNC*, and *GNL*.

HAN Negatively Regulates GATA3 Transcription Factor Expression

The expression data and genetic analysis imply that HAN may function as a negative regulator that modulates its own expression and that of other GATA3 family genes. To further test this possibility, we examined the expression of GATA3 family genes in the loss-of-function *han-1* line (Figure 8). The expression patterns of *HANL2*, *GNC*, and *GNL* remain similar in the *han-1* mutant background, with expression specifically restricted to the inner three whorls in the older flower primordia (Figure 8A). Quantification of the expression by qRT-PCR revealed that transcript accumulation from *HANL2*, *GNC*, and *GNL* increases in the *han-1* floral buds compared with those of the wild type (Figure 8B), suggesting that HAN may control the expression level of its family genes to ensure proper flower development.

HAN Forms Homomers and Heteromers with GATA3 Family Proteins

The additive phenotype of the triple mutants suggested that HAN likely works with its family members to control floral development. To examine the physical interaction between these proteins, we performed a yeast two-hybrid assay. In the X-Gal colony lift assay, HAN interacts with HAN and HANL2 strongly (strong blue color) and also interacts with GNL and GNC (moderate blue color), compared with the combination with HAN and empty vector only (Figure 9), suggesting that GATA3 family proteins physically interact. To confirm the interactions between HAN and the GATA3 family proteins *in vivo*, we also performed a bimolecular fluorescence complementation (BiFC) experiment. HAN interacted with itself and with HANL2, GNC, and GNL (Figure 9; see Supplemental Figure 4 online), but not with FAMA, an unrelated bHLH protein that had been shown to form dimers with bHLH family proteins (Ohashi-Ito and Bergmann, 2006).

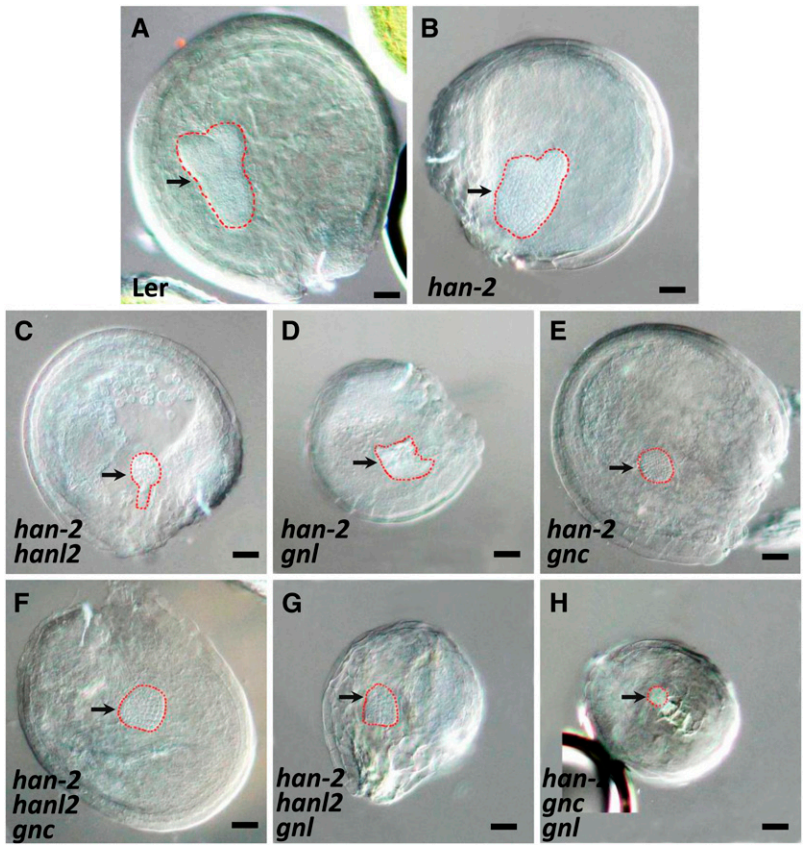

Figure 6. Embryo Development Is Defective in Double and Triple Mutants of GATA3 Family Genes.

Compared with the wild type **(A)**, the *han-2* single mutant **(B)** showed slightly defective embryos with unequal cotyledons and disordered cellular organization. Embryo development in the double (**[C]** to **[E]**) or triple mutants (**[F]** to **[H]**) of *HAN* and GATA3 family genes are mostly terminated prematurely at the globular stage, showing only a cluster of cells without proper embryo shape or organization. Arrows indicate the position of embryos, which are outlined with red, dashed lines. Bars = 50 μm.

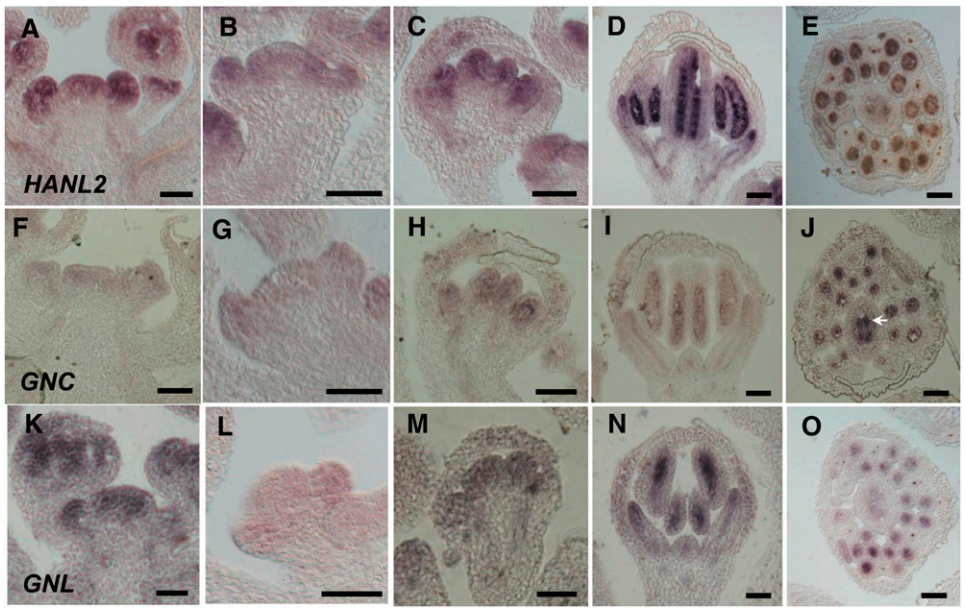

Figure 7. Similar Expression Patterns of GATA3 Family Genes in the *Arabidopsis* Flowers, as Detected by in Situ Hybridization.

The expression domains of *HANL2* (**[A]** to **[E]**), *GNC* (**[F]** to **[J]**), and *GNL* (**[K]** to **[O]**) are overlapping during wild-type flower development. Longitudinal sections of shoot apices (**[A]**, **[F]**, and **[K]**), stage 4 flowers (**[B]**, **[G]**, and **[L]**), stage 6 flowers (**[C]**, **[H]**, and **[M]**) and stage 8 flowers (**[D]**, **[I]**, and **[N]**) reveal that GATA3 family genes are expressed throughout the IM and young floral primordia (stages 1 to 3) and then limited to the inner three whorls (petal, stamen, and carpel). Transverse sections reveal that GATA3 family genes are specifically expressed in the anther locules, vascular strands, and ovules (**[E]**, **[J]**, and **[O]**). Arrow indicates the strong expression of *GNC* in the ovules within the ovary. Bars = 50 μm.

HAN Directly Binds to Its Own Promoter and the GNC Promoter in Vivo

To investigate the mechanism by which HAN repressed its own expression and that of other members of the HAN-like gene family, we performed chromatin immunoprecipitation (ChIP) experiments with anti-HAN antibody, followed by quantitative PCR analysis of the precipitated genomic DNA. We first confirmed the specificity of the anti-HAN antibody we generated. In protein gel blot analysis, the anti-HAN antibody recognized a 32-kD band in the protein extracts from wild-type flowers, but not in the protein extracts from *han1* null mutant flowers, suggesting that the anti-HAN antibody is highly specific (Figure 10A). The various amplicons used for the ChIP analyses are shown in Figure 10B, which covered different segments of the 5′ 2.5 kb of the *HAN* and *GNC* promoters. Amplicon 3 (HANp3), which spans the region from −977 to −735 bp in the *HAN* promoter, was significantly enriched, when normalized to a control using anti-actin antibody (Figure 10C). The ChIP/input ratio for amplicon 3 (HANp3) increases sixfold above a negative control amplicon from the *UBQ10* promoter in two independent biological replicates (Figure 10C). By contrast, all other amplicons from the *HAN* promoter were not enriched compared with the *UBQ10* amplicon, which demonstrated the specificity of the assay. Amplicon 3 (GNCp3) in the *GNC* promoter, which spans the region from −763 to −656 in the *GNC* promoter, was also significantly enriched, and the enrichment is up to 17-fold after normalization (Figure 10D). Amplicon 3 from −977 to −735 of the HAN promoter and amplicon 3 from the GNC promoter both contain a putative GATA consensus binding site for GATA3 family transcription factors.

DISCUSSION

HAN is a boundary-expressed GATA3 transcription factor that regulates meristem organization, flower development, and cell division (Zhao et al., 2004). The molecular mechanisms by which it performs these functions are unknown. In this study, we found that transient induction of *HAN* represses many more genes than that are induced, and genes that function in hormone responses and flower organ specification are significantly enriched among the differentially expressed genes upon *HAN* induction (Figure 1). Moreover, *HAN* induction leads to autorepression and negative regulation of the related GATA3 family genes *HANL2*, *GNC*, and *GNL* (Figure 3). Genetic analyses reveal interactions between *HAN* and GATA3 family members in the regulation of sepal separation, petal number, silique length, and stamen and embryo development (Figures 4 to 6). *HANL2*, *GNC*, and *GNL* have similar expression patterns that are partially overlapping with the expression domain of *HAN* (Figure 7) (Zhao et al., 2004). Furthermore, we showed that the expression of GATA3 family members is slightly increased in the null mutant *han-1* (Figure 8) and that HAN can form homo- and heteromultimers with GATA3 family members (Figure 9). Finally, we show that HAN protein binds to GATA-containing elements in the *HAN* and *GNC* promoters (Figure 10). The experiments together indicate

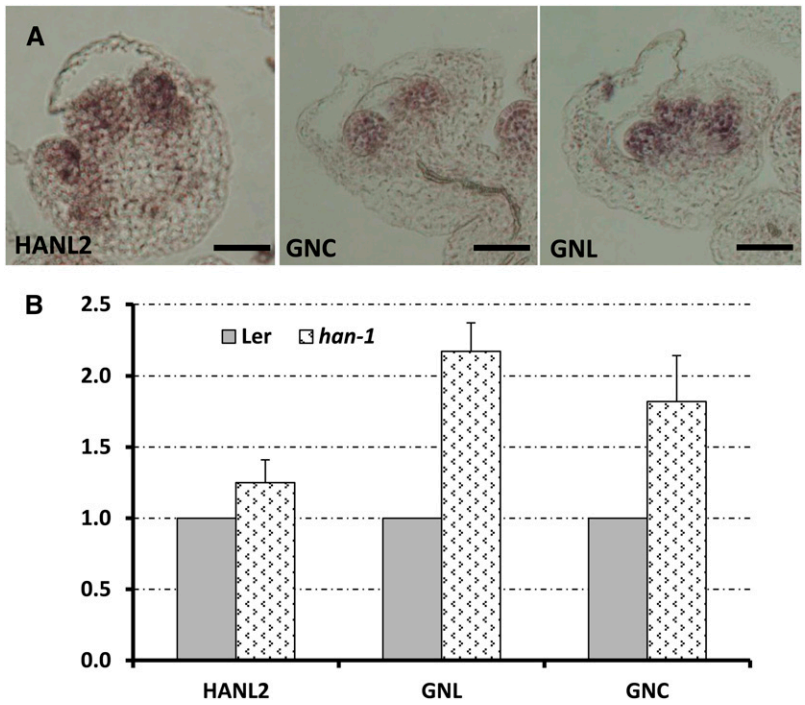

Figure 8. Transcript Accumulation from GATA3 Family Genes Is Slightly Increased in the *han-1* Loss-of-Function Mutant Background.

(A) In situ hybridization analyses showed that the expression patterns of GATA3 family genes (left, *HANL2*; middle, *GNC*; right, *GNL*) remained the same in *han-1* mutant flowers. Bars = 50 μm.

(B) qRT-PCR comparison of transcript accumulation from GATA3 family genes in L*er* and *han-1* floral buds (stages 0 to 9). Three biological replicates were performed for each gene, and all samples were normalized to *actin2*. The expression level of each gene in the L*er* background was set as 1. Bars represent the SE.

that HAN may be a repressor that modulates the spatial and temporal expression patterns of itself and other GATA3 family genes, and this protein may also regulate genes involved in hormone actions and floral organ specification to control flower development.

Autoregulation May Be a Conserved Feature for GATA Transcription Factors

The data from microarray and real-time RT-PCR analyses indicate that HAN negatively regulates its own expression (Figure 3). ChIP data suggest that this regulation is direct, with HAN binding to its own promoter (Figure 10). These data suggest a mechanism that balances HAN protein and gene expression levels through a negative feedback loop. Similarly, GATA3 family members GNC and GNL have been reported to trigger a homeostatic mechanism that controls their transcript abundance, which mediates proper GA signaling and responses, including germination, greening, leaf elongation growth, and flowering time (Richter et al., 2010). Furthermore, GATA2, a member of the subfamily I of *Arabidopsis* GATA factors, has also been shown to repress endogenous GATA2 expression in overexpression lines (Reyes et al., 2004; Luo et al., 2010). GATA2 can form a desensitizing mechanism during the light response by binding to its own promoter to feedback inhibit its transcription (Luo et al., 2010). In vertebrates, GATA factors have been shown to be involved in self-association and autoregulation as well (Crossley et al., 1995; Bates et al., 2008), suggesting that autoregulation may be a conserved feature of GATA factors. HAN also can interact with itself and several GATA3 family proteins in yeast and during a BiFC assay in transiently transformed tobacco (*Nicotiana tabacum*) cells (Figure 9; see Supplemental Figure 4 online).

GATA3 Family Genes Are Targets of HAN and Function Redundantly with HAN during Flower Development

Among the 30 members of the family of *Arabidopsis* GATA transcription factors, only mutations in the *han* gene have previously been shown to cause developmental defects in flowers (Reyes et al., 2004; Zhao et al., 2004; Bi et al., 2005). Although *GNC* and *GNL* have been shown to be directly repressed by the floral homeotic genes *APETALA3* and *PISTILLATA*, single mutants or *gnc gnl* double mutants do not show any visible flower abnormalities (Mara and Irish, 2008). Since *hanl2 gnc* or *hanl2 gnl* also do not show flower defects, we proposed that GNC, GNL, and HANL2 are functionally redundant with HAN, and their functions are largely masked by HAN activity in the wild type, since HAN directly represses and confines the expression of these genes during floral development. However, mutations in these genes can greatly enhance the phenotype of a weak *han* allele, namely, a sensitized background with reduced HAN meristem and boundary activities (Figures 4 to 6) (Zhao et al., 2004). Moreover,

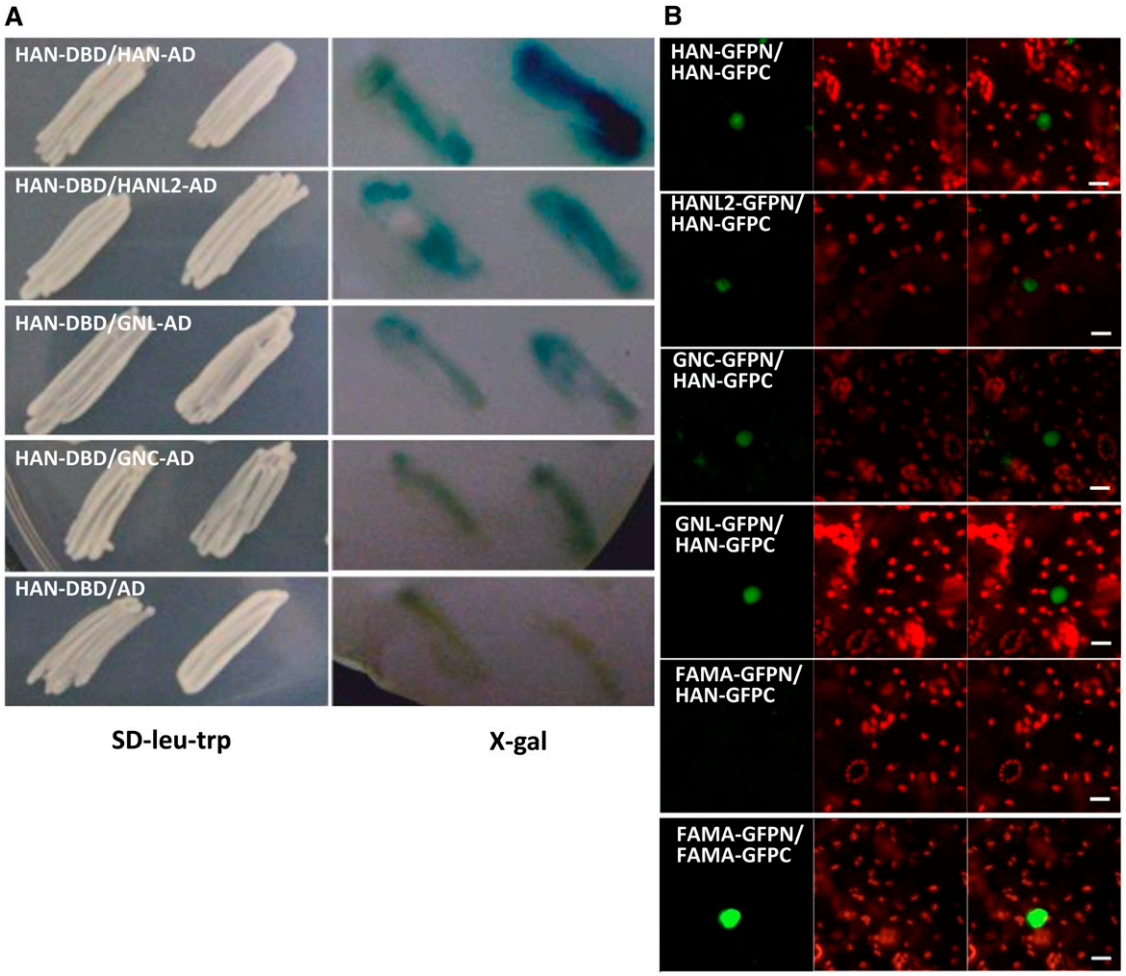

Figure 9. HAN and GATA3 Family Proteins Interact in Yeast Two-Hybrid Assays and in BiFC.

(A) Yeast two-hybrid assays. Bait constructs express HAN fused with the GAL4 DNA binding domain (DBD). Prey constructs express HAN, HANL2, GNC, or GNL fused with the GAL4 activation domain (AD). Empty prey constructs expressing the GAL4 activation domain alone serve as a negative control. Left panel shows yeast patches expressing both constructs derived from independent transformed colonies, which were streaked onto SD-Leu-Trp selection plates. Right panel indicates the X-Gal–based colony lift yeast two-hybrid assay. Blue color indicates the cumulative β-galactosidase activity caused by the activation of the lacZ reporter gene, which is activated by the physical interaction between HAN and GATA3 family proteins. At least two independent experiments were performed, and the result of one representative experiment is shown.

(B) BiFC interactions between HAN and GATA3 family proteins in transiently transformed *Nicotiana benthamiana* leaves. For each picture, a positive interaction is indicated by GFP fluorescence (green) in nuclei (left panel), the tobacco cells are indicated by chlorophyll autofluorescence (red) (middle panel), and the two merged channels are also shown (right panel). The label HAN-GFPN represents HAN fused with the N-terminal half of GFP in frame, with similar labels used for the other constructs. Representative images of different combinations, including HAN-GFPN with HAN-GFPC, HANL2-GFPN with HAN-GFPC, GNC-GFPN with HAN-GFPC, GNL-GFPN with HAN-GFPC, FAMA-GFPC with HAN-GFPC (negative control), and FAMA-GFPN with FAMA-GFPC (positive control) (Ohashi-Ito and Bergmann, 2006), are shown. All pictures were taken using the same settings, and each interaction was confirmed three times with independent infiltrations. Bars = 20 μm.

our genetic data suggest that GATA3 family members have distinct and redundant functions, in which *HANL2* and *GNL* contribute mainly to sepal separation and petal number, while *GNC* participates in stamen and carpel development in addition to sepal separation and petal number (Figures 4 and 5). The more abundant expression of *GNC* than *HANL2* and *GNL* in stamens and carpels (arrow in Figure 7J) is consistent with the prominent function of *GNC* in stamen/carpel separation. The level of gene transcript accumulation also displays similarity as well as specificity in HAN null allele *han-1* and *han-2 hanl2 gnc* triple mutant plants (see Supplemental Table 1 online). For example, TCP family transcription factor4 (TCP4) RNA exhibits a reduction in both *han-1* and *han-2 hanl2 gnc*, with a greater level of reduction in *han-1* than in *han-2 hanl2 gnc*. Similarly, the level of GH3.5 RNA is ninefold decreased in the *han-1* mutant flowers, whereas it remains unchanged in *han-2 hanl2 gnc*. The level of CORI3 mRNA, however, is fourfold decreased in the *han-1* mutant, but it is threefold increased in *han-2 hanl2 gnc*, suggesting that HAN and GATA3 family genes only share partial downstream targets.

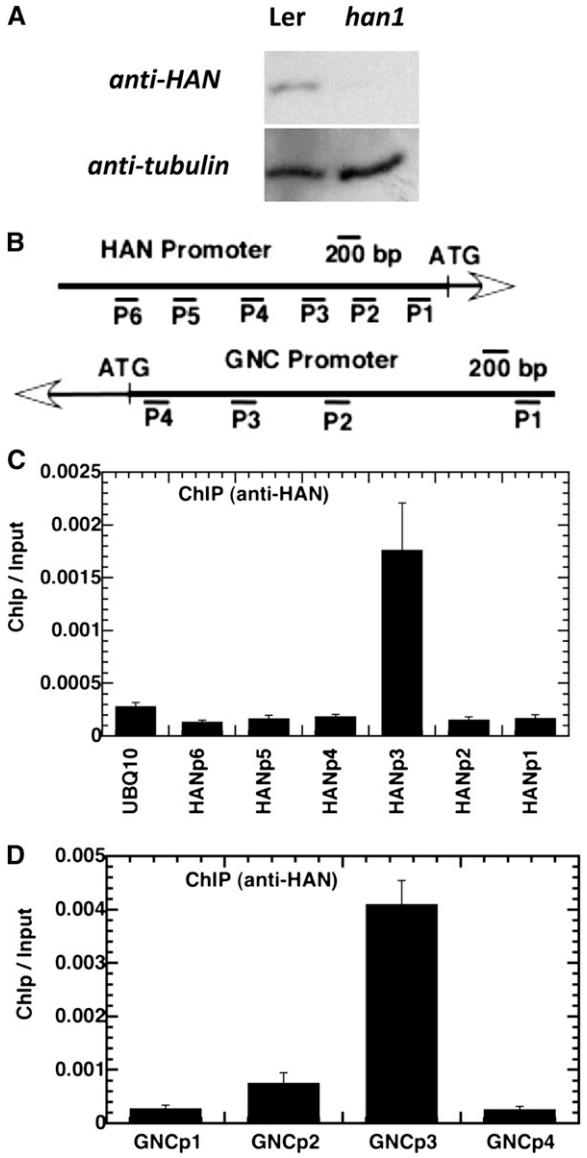

Figure 10. ChIP Analyses Indicate That HAN Directly Associates with Its Own Promoter and with That of *GNC*.

(A) Protein gel blot analyses of the specificity of binding of anti-HAN antibody in wild-type (L*er*) and *han1* floral buds.

(B) Schematic diagram of the amplicons located in the *HAN* and *GNC* promoters used for ChIP analysis.

(C) and **(D)** *HAN* **(C)** and *GNC* **(D)** chromatin regions associated with HAN protein. Quantitative data from real-time PCR show the relative enrichment value for each amplicon immunoprecipitation with anti-HAN antibody normalized to the control, in which the anti-actin antibody was used. The data presented as ChIP/input ratio were from two independent ChIP analyses of wild-type plants and were calculated for each amplicon using the following equation: ChIP/input = $2^{(Ct(MOCK) - Ct(HAN\text{-}ChIP))}/2^{(Ct(MOCK) - Ct(INPUT))}$. Error bars represent the SE from different biological replicates.

HAN May Function as a Transcription Repressor That Triggers a Feedback Mechanism

Our microarray and qRT-PCR data showed that overexpression of *HAN* leads to reduced expression of *HAN* and GATA3 family genes (Figure 3), whereas in the *han-1* null mutants, transcripts of GATA3 family genes *HANL2*, *GNC*, and *GNL* are slightly increased (Figure 8), supporting the notion that HAN may act as a transcriptional repressor during flower development. HAN is likely a negative regulator of cell growth as well, which is supported by the fact that many cell cycle genes and expansin genes, such as *CYCLIN DELTA-1* (*CYCD1;1*) and *ARABIDOPSIS THALIANA EXPANSIN A1* (*ATEXPA1*), are significantly repressed upon *HAN* overexpression (Table 3). Furthermore, plants with overaccumulation of HAN protein, such as *35S*:*HAN* or DEX-treated *35S*:*HAN-GR* lines, have reduced growth (Zhao et al., 2004). Taken together, the evidence suggests a model for HAN function (Figure 11), where in wild-type plants, HAN interacts with itself and the genes in the GATA3 family, which feeds back on the transcription of *HAN*, *HANL2*, *GNC*, and *GNL* to allow their expression at levels that are appropriate for the production of plants with normal development (Figure 11A). Transient overexpression of HAN will greatly enhance the transcriptional repression, resulting in reduced expression of *HAN* and GATA3 family genes. Such reduction is so deleterious to plant development that these plants die after ~10 d of DEX treatment (Zhao et al., 2004) (Figure 11B). In the *han* mutant background, on the other hand, reduced HAN protein levels result in weaker transcriptional repression and higher *HANL2*, *GNC*, and *GNL* expression (Figures 8 and 11C). However, the transcriptional reduction in overexpression lines, with only slight increases in the *han* null mutant background, suggest that there is an alternate repressor that functions independently of HAN to modulate the expression of GATA3 family genes, which in turn leads to plants with floral developmental defects (Figure 11C). Our quantitative PCR data support this model (Table 3). Gene expression patterns are similar in *han-1* and DEX-treated 35S:*HAN-GR* lines, suggesting that transient overexpression of HAN mimics the loss-of-function line *han1* through self-repression. Moreover, the quantitative RNA level changes are generally larger in the DEX-treated plants than in *han-1* (Table 3), which is consistent with the stronger phenotypic effect observed in the overexpression of HAN than in *han-1* plants.

HAN Regulates Flower Development via Multiple Regulatory Networks

Transient induction of HAN results in the repression of a large number of genes involved in auxin response, jasmonic acid signaling, gibberellin signaling, cytokinin response, floral organ specification, reproductive regulation, and GATA3 family genes as well (Figures 1 and 3). Biochemical analyses indicate that HAN can directly interact with itself and GATA3 family members, both at the protein level and at the DNA level (Figures 9 and 10), and the expression domains of *HAN* and GATA3 family members are partially overlapping. Considering that GATA3 family genes *GNC* and *GNL* mediate many similar pathways, including

gibberellin signaling, cytokinin response, light response, nitrogen metabolism, sugar sensing, and chlorophyll biosynthesis, and that *GNC* and *GNL* regulate genes in the *AP3/PI* pathway (Bi et al., 2005; Naito et al., 2007; Mara and Irish, 2008; Richter et al., 2010), *HAN* may function partially through *GNC* and *GNL* in boundary regions to control hormone signaling and nutrient distribution, thus ensuring proper flower separation and specification. It is also possible that HAN directly regulates hormonal response genes in the boundary regions, which in turn affect the floral organ number, size, and position. Given the complex interaction between auxin, jasmonate, gibberellin, and cytokinin during plant development, further study is needed to elucidate which, if any, hormone pathway is directly regulated by HAN (Khan and Stone, 2007; Moubayidin et al., 2009; Peng, 2009; Bishopp et al., 2011). HAN may control flower development via direct interactions with well-known floral organ regulators as well (Table 3). *BOP*, *RBE*, and *CUC3* have overlapping expression with *HAN* in the boundary regions, and *BP* and *KNAT2* share expression domain with *HAN* at the lower halves of SAMs and in carpels, respectively, while *FUS3* has an overlapping expression region with *HAN* in the embryo, indicating the possibility that the floral and embryo defects seen in the *han* mutant plants result in part from changes in the expression of these developmental regulators (Pautot et al., 2001; Vroemen et al., 2003; Takeda et al., 2004; Tsuchiya et al., 2004; Zhao et al., 2004; Hepworth et al., 2005; Hibara et al., 2006) . Future work should examine how boundary-expressing HAN interacts with hormone signaling and floral organ specification pathways during flower development.

METHODS

Plant Materials and Growth Conditions

Plants used for microarray experiments were *35S:HAN-GR* lines in the L*er* background. The *han-1* and *han-2* alleles are in the Wassilewskija and L*er* ecotypes, respectively (Zhao et al., 2004). The mutant lines of *HANL2* (SALK_138626), *GNC* (SALK_001778), and *GNL* (SALK_003995) are in the Columbia background. Double and triple mutant plants between *HAN* and GATA3 family genes with the *er* mutation were chosen for genetic and morphological analyses. All of the phenotypes were confirmed from multiple segregation lines, which rule out the effects of the ecotype. Plants were grown in a soil:vermiculite:perlite mixture under continuous illumination with a light intensity range of 80 to 100 $\mu mol \cdot m^{-2} \cdot s^{-1}$ at 20°C.

Sample Collection and Microarray Analysis

Arabidopsis thaliana inflorescences containing flower buds from stages 1 to 9 were collected for microarray analysis 0, 4, 12, and 72 h after 10 μM DEX treatment. DEX solution was made and applied every 24 h as previously described (Wellmer et al., 2006). Total RNA was extracted with TRIZOL (Invitrogen) and purified with an RNeasy kit (Qiagen). Isolated RNA was assessed for integrity using an Agilent 2100 Bioanalyzer. RNA samples from mock- and DEX-treated plants at each time point were cohybridized, and labeling dyes were swapped between replicates to reduce dye-related bias.

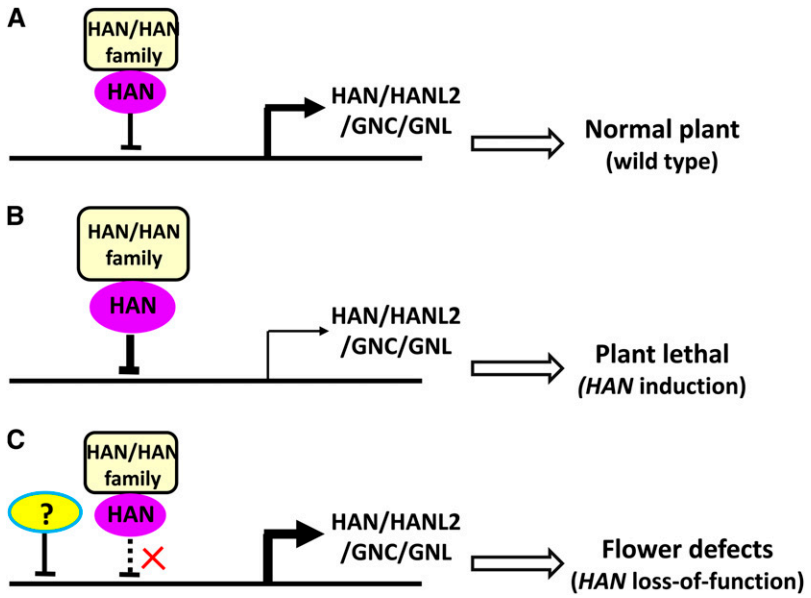

Figure 11. A Model for HAN Function in *Arabidopsis*.

(A) In the wild-type plant, HAN interacts with itself and with its family genes in a negative feedback loop, which decreases the transcription of *HAN*, *HANL2*, *GNC*, and *GNL* to produce the moderate level of expression necessary for normal plant development.

(B) Transient overexpression of HAN enhances transcriptional repression, which results in substantially reduced expression of endogenous *HAN* and GATA3 family genes and therefore has deleterious effects on plant development.

(C) In the *han* mutant background, reduced HAN protein levels result in weakened transcriptional repression and higher *HANL2*, *GNC*, and *GNL* expression. The levels are not much higher than in wild-type plants, which may indicate that an alternative (and unknown) repressor is triggered to down-modulate the expression of GATA3 family genes, producing a plant with floral developmental defects, but not complete deregulation of the GATA3 family genes.

Four biological replicates were used for microarray hybridization. Microarray labeling and hybridization were performed as described (Wellmer et al., 2004, 2006). Microarrays were scanned with a GenePix 4200A scanner (Axon Instruments), and raw data were analyzed using the Resolver gene expression data analysis system version 4.0 (Rosetta Biosoftware) as described previously (Wellmer et al., 2004, 2006). Briefly, we first removed spots that were flagged during data acquisition by Genepix software or had intensities in both channels below zero after background subtraction. We then normalized the signal intensities as described (Schadt et al., 2001). To calculate P values, we combined additive and multiplicative error components in both channels and loaded the resultant ratio profiles into the Resolver system. Analysis within the Resolver system was performed at the sequence level as described (Stoughton and Dai, 2002). If multiple data points corresponded to the same gene, their values were combined using a weighted scheme such that the feature with the lowest error was given the greatest weight. The P values calculated with Resolver were adjusted with the Benjamini and Hochberg procedure using the Bioconductor multtest package (http://www.bioconductor.org/packages/bioc/stable/src/contrib/html/multtest.html). The data are deposited in the National Center for Biotechnology Information Gene Expression Omnibus database under accession number GSE38658.

GO Term Enrichment Analysis

We clustered genes with similar expression patterns using the clustering algorithm in Resolver as described previously (Sugimoto et al., 2010). To determine which categories of genes were enriched in each cluster, we tested for enrichment of GO terms using GOEAST software (Zheng and Wang, 2008) with default parameters except for the use of algorithms to eliminate local dependencies between GO terms (Alexa et al., 2006).

Live Imaging of IMs

All imaging was performed using a Zeiss LSM 510 Meta confocal microscope with a ×40 water-dipping objective lens. Similar settings of laser power and filters were used for imaging of GFP/VENUS combination as previously described (Heisler et al., 2005). Zeiss LSM software was used for reconstructing the Z-stacks into a projection view.

Quantitative Real-Time RT-PCR

qRT-PCR analyses were first performed on cDNA synthesized from independently generated samples that were either mock- or DEX-treated for 4, 12, 72, or 9 d, using 2XsensiMix SYBR Mastermix (Bioline). Then, qRT-PCR analyses were compared using stage 0 to 9 flower buds of L*er* (control), *han-1*, *han2*, and *han-2 hanl2 gnc* mutant backgrounds. Three biological replicates were used, upon which three technical replicates were performed. Actin2 was used as a control to normalize the expression data. Fold change was calculated as $2^{\Delta\Delta Ct}$ (cycle threshold), and standard deviation was calculated among three biological replicates. The gene-specific primers are listed in Supplemental Table 2 online.

In Situ Hybridization

Tissue fixation and in situ hybridizations were performed as described (Zhang et al., 2007) with minor modifications. Western Blue plus 1 mM tetramisole was used instead of 5-Bromo-4-Chloro-3-Indolyl Phosphate/Nitroblue tetrazolium as the substrate solution to reduce the hybridization background. In situ probes were synthesized by PCR amplification of cDNA using gene-specific primers containing T7 and SP6 RNA polymerase binding sites. Antisense probes were generated using T7 RNA polymerase, and sense probes were made using SP6 RNA polymerase. The gene primer pairs are listed in Supplemental Table 2 online.

Embryo Clearing

Similar developmental stages of immature seeds were cleared with Hoyer's clearing buffer (2.5 g gum arabic, 33.3 g chloral hydrate, and 1.66 g glycerol in 10 mL water) and examined with a differential interference contrast microscope as described (Lukowitz et al., 2004).

Yeast Two-Hybrid and BiFC Assays

Yeast transformation and X-Gal–based β-galactosidase assays were performed following the manufacturer's instructions. Full-length cDNAs for *HAN*, *HANL2*, *GNC*, and *GNL* were cloned into pENTR/D/TOPO and then Gateway cloned to pDEST32 and pDEST22 through the LR reaction (Invitrogen). The bait and prey vectors were transformed to yeast strain MaV203, and three single transformed colonies were picked and streaked onto yeast peptone dextrose adenine plates for the X-Gal colony lift assay, as described in the yeast protocols handbook from Clontech. For BiFC experiments, full-length *HAN*, *HANL2*, *GNL*, and *GNC* cDNA (without stop codon) Gateway clones were recombined into vectors containing each half of *GFP* (N or C terminus) to generate the fusion proteins (such as HAN-GFP N terminus) in frame (Walter et al., 2004). Two plasmids for testing the specific interaction were co-transformed into *Nicotiana benthamiana* leaves through *Agrobacterium tumefaciens* infiltration as previously described (Lavy et al., 2002). The tobacco leaves were imaged on a Zeiss LSM 510 Meta confocal microscope 2 d after infiltration. GFP signals in nuclei (which demonstrate the physical interaction) and chlorophyll autofluorescence signals (which indicate tobacco cells) were detected at the same time from different detection channels. FAMA constructs, which have been shown to form homodimers, were included as positive controls for specificity (Ohashi-Ito and Bergmann, 2006).

Protein Expression and Antibody Preparation

Full-length HAN cDNA was cloned into the pET28-a vector to express 6xHIS-HAN protein in *Escherichia coli* RosettaBlue competent cells (Novagen). The recombinant fusion protein was purified using Ni-NTA agarose beads (Qiagen) and was used to generate polyclonal HAN antisera in rabbits by the Strategic Biosolution Company.

Protein Gel Blot Analysis

Floral buds were ground in liquid nitrogen, and proteins were extracted using a plant total protein extraction kit (Sigma-Aldrich). SDS-PAGE, blotting, and detection were performed as described (Zhang et al., 2005), with HAN or tubulin antibodies at dilutions of 1:12,000 or 1:3000, respectively, and anti-rabbit or anti-mouse secondary antibodies at a dilution of 1:2000 (Amersham). The HAN antibody recognizes the native HAN specifically as a 32-kD band (Figure 10A).

ChIP

The association of HAN with the *HAN* and *GNC* promoters was investigated in planta using ChIP, followed by a quantitative real-time PCR approach, as described (Bowler et al., 2004; Sawa et al., 2007; Zhou et al., 2009) with some modifications. In general, 2 g of shoot apex from L*er* wild-type plants was harvested and fixed with 1% formaldehyde under vacuum. Nuclei were isolated and lysed, and chromatin was sheared to an average size of 500 bp by sonication. The sonicated chromatin served as input or positive control. Immunoprecipitations were performed with anti-HAN antibody and using anti-actin antibody (Promega) as a control. The precipitated DNA was isolated and purified and served as a template for PCR. Quantitative PCR was performed as described for real-time PCR analysis. The degree of enrichment of the *HAN* or *GNC* promoter fragments was presented as the ChIP/input ratio, normalized to the antiactin control. The value was calculated as for each amplicon using following the equation $2^{(Ct(MOCK) - Ct(HAN\text{-}ChIP))}/2^{(Ct(MOCK) - Ct(INPUT))}$. The primer pairs used in ChIP-PCR are listed in Supplemental Table 2 online.

Accession Numbers

Sequence data from this article can be found in the Arabidopsis Genome Initiative databases under the following accession numbers: *HAN* (AT3G50870), *HANL2* (AT4G36620), *GNC* (AT5G56860), and *GNL* (AT4G26150).

Supplemental Data

The following materials are available in the online version of this article.

Supplemental Figure 1. Gene Ontology Term Enrichment ($P < 0.003$) in Cluster 1, Cluster 2, Cluster 3, and cluster 4 of Differentially Expressed Genes.

Supplemental Figure 2. Seed Yield Is Greatly Reduced in the Combinatory Mutants of *HAN* and GATA3 Family Genes.

Supplemental Figure 3. In Situ Hybridization of *HANL2* in *hanl2* Mutant Flowers.

Supplemental Figure 4. Negative Controls for Interactions between HAN and GATA3 Family Proteins in BiFC Experiments in Transiently Transformed *Nicotiana benthamiana* Leaves.

Supplemental Table 1. Gene Expression Patterns of Five Non-GATA HAN Targets in Mutant Plants and in the Transient Overexpression of HAN Plants.

Supplemental Table 2. Primer Information Used in This Study.

Supplemental Data Set 1. List of Genes That Are Differentially Expressed under Transient Overexpression of *HAN*.

ACKNOWLEDGMENTS

We thank members of the Meyerowitz lab for the discussion and technique help. We thank Xuemei Chen and Xigang Liu for help with the in situ hybridization, Wolfgang Lukowitz for communicating unpublished information, Arnavaz Garda for technical assistance, Adrienne Roeder for sharing constructs before publication, and Adrienne Roeder, Kaoru Sugimoto, An Yan, and Zachary Nimchuk for critical reading and comments on the article. This work was supported by National Institutes of Health Grant 1R01 GM086639 to E.M.M., by the National Basic Research of China 973 Program 2012CB113900 and National Natural Science Foundation of China 31171399 to X.Z., and by a California Institute of Technology Gosney Postdoctoral Fellowship to Y.Z.

AUTHOR CONTRIBUTIONS

X.Z. and Y.Z. conceived and performed most of the experiments and wrote the article along with E.M.M. L.D. did the real-time PCR for data verification. Z.W. and R.L. performed the microarray data analyses.

Received November 29, 2012; revised November 29, 2012; accepted December 28, 2012; published January 18, 2013.

REFERENCES

Aida, M., Ishida, T., Fukaki, H., Fujisawa, H., and Tasaka, M. (1997). Genes involved in organ separation in *Arabidopsis*: An analysis of the cup-shaped cotyledon mutant. Plant Cell **9:** 841–857.

Alexa, A., Rahnenführer, J., and Lengauer, T. (2006). Improved scoring of functional groups from gene expression data by decorrelating GO graph structure. Bioinformatics **22:** 1600–1607.

Bates, D.L., Chen, Y., Kim, G., Guo, L., and Chen, L. (2008). Crystal structures of multiple GATA zinc fingers bound to DNA reveal new insights into DNA recognition and self-association by GATA. J. Mol. Biol. **381:** 1292–1306.

Bi, Y.M., Zhang, Y., Signorelli, T., Zhao, R., Zhu, T., and Rothstein, S. (2005). Genetic analysis of *Arabidopsis* GATA transcription factor gene family reveals a nitrate-inducible member important for chlorophyll synthesis and glucose sensitivity. Plant J. **44:** 680–692.

Bishopp, A., Benková, E., and Helariutta, Y. (2011). Sending mixed messages: Auxin-cytokinin crosstalk in roots. Curr. Opin. Plant Biol. **14:** 10–16.

Bowler, C., Benvenuto, G., Laflamme, P., Molino, D., Probst, A.V., Tariq, M., and Paszkowski, J. (2004). Chromatin techniques for plant cells. Plant J. **39:** 776–789.

Bowman, J.L., Smyth, D.R., and Meyerowitz, E.M. (1991). Genetic interactions among floral homeotic genes of *Arabidopsis*. Development **112:** 1–20.

Brewer, P.B., Howles, P.A., Dorian, K., Griffith, M.E., Ishida, T., Kaplan-Levy, R.N., Kilinc, A., and Smyth, D.R. (2004). PETAL LOSS, a trihelix transcription factor gene, regulates perianth architecture in the *Arabidopsis* flower. Development **131:** 4035–4045.

Chuang, C.F., Running, M.P., Williams, R.W., and Meyerowitz, E.M. (1999). The *PERIANTHIA* gene encodes a bZIP protein involved in the determination of floral organ number in *Arabidopsis thaliana*. Genes Dev. **13:** 334–344.

Clark, S.E., Williams, R.W., and Meyerowitz, E.M. (1997). The *CLAVATA1* gene encodes a putative receptor kinase that controls shoot and floral meristem size in *Arabidopsis*. Cell **89:** 575–585.

Coen, E.S., and Meyerowitz, E.M. (1991). The war of the whorls: Genetic interactions controlling flower development. Nature **353:** 31–37.

Crossley, M., Merika, M., and Orkin, S.H. (1995). Self-association of the erythroid transcription factor GATA-1 mediated by its zinc finger domains. Mol. Cell. Biol. **15:** 2448–2456.

De Rybel, B., et al. (2010). A novel aux/IAA28 signaling cascade activates GATA23-dependent specification of lateral root founder cell identity. Curr. Biol. **20:** 1697–1706.

Durfee, T., Roe, J.L., Sessions, R.A., Inouye, C., Serikawa, K., Feldmann, K.A., Weigel, D., and Zambryski, P.C. (2003). The F-box-containing protein UFO and AGAMOUS participate in antagonistic pathways governing early petal development in *Arabidopsis*. Proc. Natl. Acad. Sci. USA **100:** 8571–8576.

Fletcher, J.C. (2002). Shoot and floral meristem maintenance in *Arabidopsis*. Annu. Rev. Plant Biol. **53:** 45–66.

Fletcher, J.C., Brand, U., Running, M.P., Simon, R., and Meyerowitz, E.M. (1999). Signaling of cell fate decisions by CLAVATA3 in *Arabidopsis* shoot meristems. Science **283:** 1911–1914.

Fonseca, S., Chico, J.M., and Solano, R. (2009). The jasmonate pathway: The ligand, the receptor and the core signalling module. Curr. Opin. Plant Biol. **12:** 539–547.

Heisler, M.G., Ohno, C., Das, P., Sieber, P., Reddy, G.V., Long, J.A., and Meyerowitz, E.M. (2005). Patterns of auxin transport and gene expression during primordium development revealed by live imaging of the *Arabidopsis* inflorescence meristem. Curr. Biol. **15:** 1899–1911.

Hepworth, S.R., Zhang, Y., McKim, S., Li, X., and Haughn, G.W. (2005). BLADE-ON-PETIOLE-dependent signaling controls leaf and floral patterning in *Arabidopsis*. Plant Cell **17:** 1434–1448.

Hibara, K., Karim, M.R., Takada, S., Taoka, K., Furutani, M., Aida, M., and Tasaka, M. (2006). *Arabidopsis* CUP-SHAPED COTYLEDON3 regulates postembryonic shoot meristem and organ boundary formation. Plant Cell **18:** 2946–2957.

Hirano, K., Ueguchi-Tanaka, M., and Matsuoka, M. (2008). GID1-mediated gibberellin signaling in plants. Trends Plant Sci. **13:** 192–199.

Kanei, M., Horiguchi, G., and Tsukaya, H. (2012). Stable establishment of cotyledon identity during embryogenesis in *Arabidopsis* by ANGUSTIFOLIA3 and HANABA TARANU. Development **139:** 2436–2446.

Khan, S., and Stone, J.M. (2007). *Arabidopsis thaliana* GH3.9 in auxin and jasmonate cross talk. Plant Signal. Behav. **2:** 483–485.

Lavy, M., Bracha-Drori, K., Sternberg, H., and Yalovsky, S. (2002). A cell-specific, prenylation-independent mechanism regulates targeting of type II RACs. Plant Cell **14:** 2431–2450.

Liu, P.P., Koizuka, N., Martin, R.C., and Nonogaki, H. (2005). The BME3 (Blue Micropylar End 3) GATA zinc finger transcription factor is a positive regulator of *Arabidopsis* seed germination. Plant J. **44:** 960–971.

Long, J.A., Moan, E.I., Medford, J.I., and Barton, M.K. (1996). A member of the KNOTTED class of homeodomain proteins encoded by the STM gene of *Arabidopsis*. Nature **379:** 66–69.

Lowry, J.A., and Atchley, W.R. (2000). Molecular evolution of the GATA family of transcription factors: Conservation within the DNA-binding domain. J. Mol. Evol. **50:** 103–115.

Lukowitz, W., Roeder, A., Parmenter, D., and Somerville, C. (2004). A MAPKK kinase gene regulates extra-embryonic cell fate in *Arabidopsis*. Cell **116:** 109–119.

Luo, X.M., et al. (2010). Integration of light- and brassinosteroid-signaling pathways by a GATA transcription factor in *Arabidopsis*. Dev. Cell **19:** 872–883.

Mara, C.D., and Irish, V.F. (2008). Two GATA transcription factors are downstream effectors of floral homeotic gene action in *Arabidopsis*. Plant Physiol. **147:** 707–718.

Mayer, K.F., Schoof, H., Haecker, A., Lenhard, M., Jürgens, G., and Laux, T. (1998). Role of WUSCHEL in regulating stem cell fate in the *Arabidopsis* shoot meristem. Cell **95:** 805–815.

Moubayidin, L., Di Mambro, R., and Sabatini, S. (2009). Cytokinin-auxin crosstalk. Trends Plant Sci. **14:** 557–562.

Naito, T., Kiba, T., Koizumi, N., Yamashino, T., and Mizuno, T. (2007). Characterization of a unique GATA family gene that responds to both light and cytokinin in *Arabidopsis thaliana*. Biosci. Biotechnol. Biochem. **71:** 1557–1560.

Nawy, T., Bayer, M., Mravec, J., Friml, J., Birnbaum, K.D., and Lukowitz, W. (2010). The GATA factor HANABA TARANU is required to position the proembryo boundary in the early *Arabidopsis* embryo. Dev. Cell **19:** 103–113.

Ohashi-Ito, K., and Bergmann, D.C. (2006). *Arabidopsis* FAMA controls the final proliferation/differentiation switch during stomatal development. Plant Cell **18:** 2493–2505.

Patient, R.K., and McGhee, J.D. (2002). The GATA family (vertebrates and invertebrates). Curr. Opin. Genet. Dev. **12:** 416–422.

Pautot, V., Dockx, J., Hamant, O., Kronenberger, J., Grandjean, O., Jublot, D., and Traas, J. (2001). KNAT2: Evidence for a link between knotted-like genes and carpel development. Plant Cell **13:** 1719–1734.

Pelaz, S., Ditta, G.S., Baumann, E., Wisman, E., and Yanofsky, M.F. (2000). B and C floral organ identity functions require SEPALLATA MADS-box genes. Nature **405:** 200–203.

Peng, J. (2009). Gibberellin and jasmonate crosstalk during stamen development. J. Integr. Plant Biol. **51:** 1064–1070.

Putterill, J., Robson, F., Lee, K., Simon, R., and Coupland, G. (1995). The *CONSTANS* gene of *Arabidopsis* promotes flowering and encodes a protein showing similarities to zinc finger transcription factors. Cell **80:** 847–857.

Reyes, J.C., Muro-Pastor, M.I., and Florencio, F.J. (2004). The GATA family of transcription factors in *Arabidopsis* and rice. Plant Physiol. **134:** 1718–1732.

Richter, R., Behringer, C., Müller, I.K., and Schwechheimer, C. (2010). The GATA-type transcription factors GNC and GNL/CGA1 repress gibberellin signaling downstream from DELLA proteins and PHYTOCHROME-INTERACTING FACTORS. Genes Dev. **24:** 2093–2104.

Sakai, H., Medrano, L.J., and Meyerowitz, E.M. (1995). Role of SUPERMAN in maintaining *Arabidopsis* floral whorl boundaries. Nature **378:** 199–203.

Sawa, M., Nusinow, D.A., Kay, S.A., and Imaizumi, T. (2007). FKF1 and GIGANTEA complex formation is required for day-length measurement in *Arabidopsis*. Science **318:** 261–265.

Scazzocchio, C. (2000). The fungal GATA factors. Curr. Opin. Microbiol. **3:** 126–131.

Schadt, E.E., Li, C., Ellis, B., and Wong, W.H. (2001). Feature extraction and normalization algorithms for high-density oligonucleotide gene expression array data. J. Cell Biochem. Suppl. **37:** 120–125.

Stoughton, R.S., and Dai, H. (2002). Statistical combining of cell expression profiles. U.S. Patent 6351712.

Sugimoto, K., Jiao, Y., and Meyerowitz, E.M. (2010). *Arabidopsis* regeneration from multiple tissues occurs via a root development pathway. Dev. Cell **18:** 463–471.

Sugimoto, K., Takeda, S., and Hirochika, H. (2003). Transcriptional activation mediated by binding of a plant GATA-type zinc finger protein AGP1 to the AG-motif (AGATCCAA) of the wound-inducible Myb gene NtMyb2. Plant J. **36:** 550–564.

Takeda, S., Matsumoto, N., and Okada, K. (2004). RABBIT EARS, encoding a SUPERMAN-like zinc finger protein, regulates petal development in *Arabidopsis thaliana*. Development **131:** 425–434.

Teakle, G.R., Manfield, I.W., Graham, J.F., and Gilmartin, P.M. (2002). *Arabidopsis thaliana* GATA factors: Organisation, expression and DNA-binding characteristics. Plant Mol. Biol. **50:** 43–57.

To, J.P., and Kieber, J.J. (2008). Cytokinin signaling: Two-components and more. Trends Plant Sci. **13:** 85–92.

Tsuchiya, Y., Nambara, E., Naito, S., and McCourt, P. (2004). The FUS3 transcription factor functions through the epidermal regulator TTG1 during embryogenesis in *Arabidopsis*. Plant J. **37:** 73–81.

Vroemen, C.W., Mordhorst, A.P., Albrecht, C., Kwaaitaal, M.A., and de Vries, S.C. (2003). The CUP-SHAPED COTYLEDON3 gene is required for boundary and shoot meristem formation in *Arabidopsis*. Plant Cell **15:** 1563–1577.

Walter, M., Chaban, C., Schutze, K., Batistic, O., Weckermann, K., Nake, C., Blazevic, D., Grefen, C., Schumacher, K., Oecking, C., Harter, K., and Kudla, J. (2004). Visualization of protein interactions in living plant cells using bimolecular fluorescence complementation. Plant J. **40:** 428–438.

Wang, H., Tian, C.-e., Duan, J., and Wu, K. (2008). Research progresses on GH3s, one family of primary auxin-responsive genes. Plant Growth Regul. **56:** 225–232.

Wang, L., Yin, H., Qian, Q., Yang, J., Huang, C., Hu, X., and Luo, D. (2009). NECK LEAF 1, a GATA type transcription factor, modulates organogenesis by regulating the expression of multiple regulatory genes during reproductive development in rice. Cell Res. **19:** 598–611.

Weigel, D., and Meyerowitz, E.M. (1994). The ABCs of floral homeotic genes. Cell **78:** 203–209.

Wellmer, F., Alves-Ferreira, M., Dubois, A., Riechmann, J.L., and Meyerowitz, E.M. (2006). Genome-wide analysis of gene expression during early *Arabidopsis* flower development. PLoS Genet. **2:** e117.

Wellmer, F., Riechmann, J.L., Alves-Ferreira, M., and Meyerowitz, E.M. (2004). Genome-wide analysis of spatial gene expression in *Arabidopsis* flowers. Plant Cell **16:** 1314–1326.

Whipple, C.J., Hall, D.H., DeBlasio, S., Taguchi-Shiobara, F., Schmidt, R.J., and Jackson, D.P. (2010). A conserved mechanism of bract suppression in the grass family. Plant Cell **22:** 565–578.

Zhang, W., Sun, Y., Timofejeva, L., Chen, C., Grossniklaus, U., and Ma, H. (2006). Regulation of *Arabidopsis* tapetum development and

function by DYSFUNCTIONAL TAPETUM1 (DYT1) encoding a putative bHLH transcription factor. Development **133:** 3085–3095.

Zhang, X., Li, X., Marshall, J.B., Zhong, C.X., and Dawe, R.K. (2005). Phosphoserines on maize CENTROMERIC HISTONE H3 and histone H3 demarcate the centromere and pericentromere during chromosome segregation. Plant Cell **17:** 572–583.

Zhang, X., Madi, S., Borsuk, L., Nettleton, D., Elshire, R.J., Buckner, B., Janick-Buckner, D., Beck, J., Timmermans, M., Schnable, P.S., and Scanlon, M.J. (2007). Laser microdissection of narrow sheath mutant maize uncovers novel gene expression in the shoot apical meristem. PLoS Genet. **3:** e101.

Zhao, Y., Medrano, L., Ohashi, K., Fletcher, J.C., Yu, H., Sakai, H., and Meyerowitz, E.M. (2004). HANABA TARANU is a GATA transcription factor that regulates shoot apical meristem and flower development in *Arabidopsis*. Plant Cell **16:** 2586–2600.

Zheng, Q., and Wang, X.J. (2008). GOEAST: A web-based software toolkit for Gene Ontology enrichment analysis. Nucleic Acids Res. **36**(Web Server issue)**:** W358–W363.

Zhou, Y., Zhang, X., Kang, X., Zhao, X., Zhang, X., and Ni, M. (2009). SHORT HYPOCOTYL UNDER BLUE1 associates with MINISEED3 and HAIKU2 promoters in vivo to regulate *Arabidopsis* seed development. Plant Cell **21:** 106–117.